

1 Preprint published at EarthArxiv:

2 <https://doi.org/10.31223/X54M0V>

3
4
5 Indian Plate paleogeography, subduction, and horizontal
6 underthrusting below Tibet: paradoxes, controvercies,
7 and opportunities

8
9
10 DOUWE J.J. VAN HINSBERGEN

11
12
13 Department of Earth Sciences, Utrecht University, Princetonlaan 8A, 3584 CB
14 Utrecht, the Netherlands. d.j.j.vanhinsbergen@uu.nl

15
16
17 *This is a non-peer reviewed preprint. This manuscript is submitted for publication in*
18 *NATIONAL SCIENCE REVIEW. Subsequent version of this manuscript may differ*
19 *slightly in content. Once accepted, the published version will be available through the*
20 *'peer-reviewed publication doi' on this website. Feel free to contact me with comments.*

21
22 *This is a second version, February 11, 2022. A first version (Feb 5) contained an*
23 *error in the plate circuit, and consequent estimates of convergence, which has been*
24 *corrected in version 2, including in Figures 1, 3, and 4.*

Keywords

Collision, orogenesis, subduction, reconstruction, Himalaya, Tibet

Abstract

The India-Asia collision zone is the archetype to calibrate geological responses of continent-continent collision, but hosts a paradox: there is no orogen-wide geological record of oceanic subduction after initial collision around 60-55 Ma, yet thousands of kilometers of post-collisional subduction occurred before arrival of unsubductable continental lithosphere that currently horizontally underlies Tibet. I show that kinematically restoring incipient horizontal underthrusting accurately predicts geologically estimated diachronous slab break-off, unlocking the Miocene of Himalaya-Tibet as natural laboratory for unsubductable lithosphere convergence. Additionally, three end-member paleogeographic scenarios exist with different predictions for the nature of post-collisional subducting lithosphere but each is defended and challenged based on similar data types. Here, I attempt at breaking through this impasse by identifying how the three paleogeographic scenario each challenge paradigms in geodynamics, orogenesis, magmatism, or paleogeographic reconstruction and identify opportunities for methodological advances in paleomagnetism, sediment provenance analysis, and seismology to conclusively constrain Greater Indian paleogeography.

Introduction

With major continents being too buoyant to subduct – the reason why they can become billions of years old (1) – colliding continents are associated with subduction arrest, plate reorganization, and orogenesis (2), seaway closure, mountain building, and atmospheric barrier formation (3), and exchange and diversification of terrestrial biota (4). The orogen at the India-Asia continental collision zone is the archetype to calibrate the relationships between collision, orogenic architecture, history, and dynamics, resulting magmatism and mineralization, as well as climatic and biological responses (3,

53 5-8). But long-standing paradoxes and controversies in tectonic history have led to an
54 impasse, making using the full potential of the archetype difficult.

55 Geophysical imaging has revealed that Indian continental lithosphere has
56 horizontally underthrust the Tibetan upper plate (9-14). This is consistent with the
57 paradigm of unsubductability of thick continental lithosphere (2) and offers opportunities
58 to study the dynamics of and response to convergence between buoyant lithospheres (15).
59 But Indian lithosphere only reaches ~400-800 km north of the Himalayan front (9-14)
60 and according to kinematic reconstructions of Indian plate consumption (11, 13, 16), and
61 geological estimates of the last slab break-off in the Himalaya (17), accounts for only the
62 last 25-13 Ma (diachronous along-strike) of India-Asia convergence (11, 16).
63 Paradoxically, the youngest unequivocal geological records of plate-boundary-wide
64 oceanic subduction between India and Asia are older than 60 Ma (18, 19), after which
65 more than 4000 km of India-Asia plate convergence occurred (20, 21). So between the
66 geologically recorded collision and the onset of horizontal underthrusting of Indian
67 lithosphere, thousands of kilometers of post-collisional subduction occurred.

68 This paradox is not readily explained by dynamic models of continental collision.
69 These rather portray a process of ~10 Ma, during which a few hundred kilometers of one
70 continental margin is dragged down below another, causing deformation of both margins,
71 after which convergence stops, the slab detaches, and the deformed belt rebounds and
72 uplifts (22). Long-standing controversy in the geological debate on the India-Asia
73 collision history comes from different solutions to explain this paradox. End-member
74 solutions fall into three classes that fundamentally differ in post-collisional
75 paleogeography of the Indian plate. The first end-member predicts that all post-collisional
76 subduction consumed continental lithosphere (19, 23, 24), and the second and third infer
77 that after initial collision, oceanic lithosphere remained to the north (8, 25-28), or to the
78 south (11, 29) of the initial collision zone, which subsequently subducted 'post-collision'.
79 The former option challenges the paradigm of continental unsubductability and if true, is
80 key to advance understanding of mantle dynamics (24). The latter options challenge
81 paradigms of orogenic architecture and evolution ensuing from oceanic subduction (23,
82 30) and if true, holds key lessons for reconstructing paleogeography from orogenic

83 archives (31). In all cases, the records of magmatism, deformation, and topographic rise
84 in Tibet and the Himalaya between the onset of collision and the onset of horizontal
85 underthrusting occurred in context of, and contain key information on a-typical
86 subduction, either in terms of the nature of the downgoing plate, or in terms of the
87 orogenic and magmatic response.

88 In the last decade, the controversy on India's paleogeography has reached an
89 impasse: each of the end-member scenarios is argued for and against based on the same
90 types of data, notably sediment provenance constraining upper plate sediments arriving
91 on lower plate continental margins (8, 11, 19, 27, 32, 33), paleomagnetic data
92 constraining paleolatitudes of continental margins and arcs (27, 29, 34-37), and seismic
93 tomographic images revealing locations of past subduction zones (13, 16, 38, 39). Even
94 though the volume of these databases has rapidly increased in recent years, they have
95 mostly led to repetition of these views on Indian paleogeography, and somewhat
96 distracted from using the unique opportunities of the archetype to challenge and develop
97 paradigms of geodynamics, orogenesis, and environmental response.

98 The aims of this paper are three-fold: (i) I first attempt at formulating the paradox
99 and explaining the controversy and the key predictions of each proposed class of
100 explanations; (ii) I then review geological constraints on Indian plate subduction
101 provided by the Himalayan mountains that consist of offscraped and thrust upper
102 crustal rocks derived from Indian plate lithosphere and on coeval upper plate geological
103 evolution of the Tibetan Plateau; (iii) I will use these constraints to identify which
104 tectonic and magmatic reorganizations coincide with horizontal Indian underthrusting,
105 and aim to identify the natural laboratory to analyze the dynamics of non-sudbuctable
106 lithosphere convergence; (iv) Finally, I will discuss ways forward to reconcile existing
107 datasets and find novel ones to break through the impasse in Greater India
108 paleogeography reconstruction and show the opportunities that each of the three end-
109 member scenarios would provide in using the India-Asia archetype to constrain the
110 geological and dynamic consequences of its a-typical post-collisional subduction.

111

112 Review

113 The paradox: underthrust versus subducted Indian plate lithosphere

114 A key question in the analysis of the India-Asia collision history and dynamics is
115 where and how post-collisional convergence has been accommodated. Kinematic
116 reconstructions have shown that approximately 1000-1200 km of Cenozoic convergence
117 was accommodated by shortening and extrusion in the overriding plate of Tibet (11, 40,
118 41). Reconstructing this convergence in the mantle reference frame aligns the southern
119 Eurasian margin with underlying slabs imaged by seismic tomography, and in the
120 paleomagnetic reference frame satisfies first-order vertical axis rotations and south
121 Tibetan paleolatitudes for the Cretaceous and Paleogene (11). This reconstructed
122 shortening of Tibet is by far the largest amount of intra-plate shortening recorded in post-
123 Paleozoic orogens (31). Shortening records of the Indian-plate-derived thin-skinned
124 Himalaya fold-thrust belt give somewhat smaller numbers, between 600-900 km (42). It
125 is puzzling that post-collisional convergence far exceeds these numbers: the earliest
126 estimates for post-collisional convergence assumed a 45 Ma collision and predicted a
127 shortening deficit of ~1000 km (43), but stratigraphic ages of the oldest foreland basin
128 clastics in the northernmost continental rocks of the Himalaya, as well as ages of (U)HP
129 metamorphism in continent-derived rocks in the northern Himalaya has pushed the
130 estimated initial collision age backward, to ~60-55 Ma (18, 44, 45). India-Asia plate
131 circuits constrained by magnetic anomalies predict 3500 and 4500 km of post-60 Ma
132 convergence at the longitude of the western and eastern Himalayan syntaxis, respectively
133 and (20)(21) (Fig. 1). Much of the post-collisional subduction has thus not left an
134 accreted rock record, either because of whole-sale subduction, or of (subduction-) erosion
135 of previously accreted records.

136 Seismological research in the last two decades has painted a detailed image of the
137 mantle below India and Tibet that helps identifying where lost lithosphere may now
138 reside. First, lithosphere below Tibet is up to 260 km thick, which was at first surprising
139 (46): major lithospheric thickening associated with intraplate shortening is predicted to
140 lead to convective instability of lithosphere, that will then delaminate (47). However,
141 since then the thick lithosphere below Tibet has become interpreted as horizontally
142 underthrust Indian crust and continental mantle lithosphere (9-14). Tibetan lithosphere

143 has indeed delaminated: Indian continental crust appears to directly underlie Tibetan
144 crust, not intervened by a thick lithospheric mantle (14). In addition, seismic tomographic
145 evidence for bodies of high-velocity material that may represent delaminated Tibetan
146 lithosphere have been identified in the upper mantle below the horizontally underthrust
147 Indian lithosphere, suggesting delamination prior to underthrusting (48). Moreover,
148 recent seismological analysis has shown that delamination is not restricted to Tibet, but
149 also affected the Yunnan region to the southeast of the eastern Himalayan syntaxis, where
150 a conspicuous, circular shaped hole in the continental lithosphere is underlain by a body of
151 high-velocity material at the base of the upper mantle (49).

152 The first detailed seismological section that detected horizontally underthrust
153 lithosphere revealed that the Indian continent protrudes ~400 km north of the southern
154 Himalayan front (14). Since then, multiple seismic tomography models have reproduced
155 this finding, but showed that the shape of the northern Indian margin is irregular,
156 protruding ~800 km northward at the longitude of the eastern Himalayan syntaxis,
157 abruptly stepping southward to the north of Bhutan, and then increasing to ~700 km
158 again towards the longitude of the western syntaxis (Fig. 2) (9-13). An onset of horizontal
159 underthrusting can be calculated when assuming that the body of lithosphere below Tibet
160 is a rigid part of the Indian plate, reconstructing India-Asia convergence, and corrected
161 for Tibetan shortening. This predicts that the onset of horizontal underthrusting started
162 around the Himalayan syntaxes around 28 Ma, and becomes gradually younger to ~15
163 Ma at the longitude of Bhutan (11, 16) (Fig. 3). Geological reconstructions of uplift,
164 heating, and resulting leucogranite intrusion in the Himalayan mountain range interpreted
165 to reflect lateral propagation of slab detachment a few Ma after the underthrusting of the
166 modern Indian crust below Tibet, predicted 25 Ma for the eastern- and westernmost
167 Himalaya, gradually younging towards 13 Ma in Bhutan (17). This match suggests that
168 the thick body of lithosphere below Tibet is indeed horizontally underthrust Indian
169 lithosphere.

170 All Indian plate lithosphere that was consumed before Miocene horizontal
171 underthrusting must thus have subducted into the mantle. There is broad consensus that
172 the majority of this subducted lithosphere resides in the lower mantle below India, with a

173 smaller and younger slab that was the last to detach, overturned in the mantle to the north
174 of the main India slab (Fig. 2) (11, 13, 38, 39, 50). An additional anomaly in the lower
175 mantle below the equatorial Indian ocean has also long been interpreted as Neotethyan
176 (29, 38, 39), but may instead be a relict of Mesozoic subduction between Tibetan blocks
177 (16) (Fig. 2).

178 In summary, the paradox of the India-Asia collision is the following: there is no
179 geological record of oceanic subduction along the width of the orogen after initial
180 collision around 60 Ma, and the system is therefore widely believed to have been fully
181 continental since this time (13, 23, 24); yet thousands of kilometers of Indian plate
182 lithosphere was consumed without leaving an accretionary record, and subducted deeply
183 into the mantle, which are both typically associated with oceanic subduction and not
184 previously demonstrated for continents (31). Only in the early to middle Miocene,
185 unsubductable Indian Plate lithosphere arrived in the collision zone, and horizontally
186 underthrust the upper plate.

187

188 [The controversy: scenarios for Indian plate paleogeography and subduction](#) 189 [history](#)

190 The above paradox has led to paleogeographic reconstructions for post-collisional
191 Greater India that fall into three classes (Fig. 4). The first and most commonly portrayed
192 scenario (Model C, for Continental) assumes that all post-collisional convergence
193 consumed continental lithosphere (19, 23, 24, 40). This scenario provides a
194 straightforward explanation for the absence of accretion of OPS after 60 Ma in the
195 Himalayan orogen, but requires thousands of kilometers of continental subduction, and
196 this subduction must have been accommodated along a thrust in the Himalayas (24). The
197 width of continental Greater India portrayed on published paleogeographic maps differs
198 as function of collision age, plate circuit, and assumed Tibetan shortening, but predicts
199 Gondwana reconstructions in which Greater India was conjugate to the entire western
200 Indian margin (24) up to or beyond the Argo Abyssal Plain (Fig. 4). This Argo Abyssal
201 Plain is of importance because it recorded Jurassic continental break-up, around 155 Ma,

202 well before the separation of India from Australia around 130 Ma, and was thus
203 conjugate to a different continent and plate than India: Argoland (51).

204 The second scenario (model A, for Arc) points out that between the Himalaya and
205 continental southern Eurasia, there are ophiolites and intra-oceanic arc rocks, and invokes
206 that the 60 Ma collision recorded arrival of the north Indian continental margin in an
207 intra-oceanic subduction zone, followed by obduction of ophiolites and arc rocks onto the
208 continental margin (8, 25-28, 52). Following this collision, oceanic lithosphere remained
209 between the initial collision zone and Eurasia, which was consumed until arrival of the
210 obducted Indian continental margin at the Tibetan trench. Because there is no
211 accretionary record of post-60 Ma oceanic subduction, the age of this arrival is based on
212 interpretations of changes in magmatism in Tibet, or an a (contested) youngest age of
213 marine sedimentation in the Himalaya, at 40 ± 5 Ma (8, 26, 28). To explain how Tibet-
214 derived sediments arrived at the north-Indian margin around 60 Ma, a recent modification
215 of this model suggested that the north Himalayan ophiolites originated at the south
216 Tibetan margin in the early Cretaceous, but migrated southward, together with overlying
217 Tibet-derived sediments, due to opening of a back-arc basin (8). The intra-oceanic arc
218 scenario thus predicts that part of the post-collisional subduction history consumed
219 oceanic lithosphere that must have subducted along a trench between the Himalayan
220 ophiolites and the south Tibetan margin. Additionally, the assumed 40 ± 5 Ma collision
221 age of the obducted Indian margin and Tibet would still require large amounts (up to
222 1000 km at the longitude of Bhutan) of continental subduction prior to horizontal
223 underthrusting (Fig. 4). The reconstructed width of continental Greater India depends on
224 the assumed collision age with Tibet, but would bring the north Greater Indian margin
225 adjacent to most of the west Australian margin up to the Cape Range Fracture Zone (Fig.
226 4).

227 The third scenario (model M, for Microcontinent) invokes that the 60 Ma
228 collision in the north Himalaya involves a Tibetan Himalayan microcontinent that rifted
229 and drifted away from Greater India in Cretaceous times, opening a conceptual Greater
230 India Basin (GIB) ocean in its wake (29). Assuming that the horizontally underthrust
231 portion of India below Tibet represents the southern paleo-passive margin of this basin
232 leads to a reconstruction whereby Greater India in Gondwana times did not extend

233 beyond the Wallaby Fracture Zone of the southwest Australian margin (11), far south of
234 the Argo Abyssal Plain, but consistent with west Australian margin reconstructions that
235 interpreted that Jurassic break-up of Argoland to continue to the Wallaby Fracture Zone
236 (51). This model thus invokes that continental subduction was restricted to only the lower
237 crustal and mantle underpinnings of the Tibetan Himalayan microcontinent. However,
238 this model also requires that an oceanic basin was consumed along a thrust within the
239 Himalayan mountain range without leaving a modern geological record anywhere in the
240 Himalaya. Finally, this scenario does not require, but also does not exclude the intra-
241 oceanic arc scenario of Model A – this would merely change the width of the GIB.

242 Each of these scenarios explains some first-order observations from the Greater
243 Indian paradox, and satisfies some long-held paradigms in subduction behavior or
244 orogenesis, but challenges others. And each of these models has been defended as well as
245 contested based on paleomagnetic, structural geological, stratigraphic, and seismic
246 tomographic data. Below, I will briefly review the geological architecture of the
247 Himalaya and Tibet that is relevant to identify future research targets to advance the
248 discussion, and to identify the main geological and geodynamic phenomena that occurred
249 in the time window of horizontal Indian underthrusting.

250

251 **The constraints: architecture and evolution of the Tibetan-Himalayan orogen**

252 Elements of the Himalayan and Tibetan orogen that play a key role in the
253 interpretations of its tectonic history since 60 Ma are (i) the accretionary fold-thrust belt
254 of the Himalaya that was offscraped from now-underthrust/subducted Indian plate
255 lithosphere ; (ii) a belt of overlying ophiolites, and in the west of the collision zone,
256 Cretaceous-Eocene intra-oceanic arc rocks that represent the upper plate of an overriding
257 oceanic lithosphere above a subduction zone; and (iii) continental crust of the Tibetan
258 plateau that consists of pre-Cenozoic accreted terranes and intervening sutures, intruded
259 by a Mesozoic-Cenozoic magmatic arc that also shows it was in an upper plate position
260 above a subduction zone (Fig. 5). Below, I summarize these constraints and briefly
261 indicate how they play a role in the three scenarios for Indian paleogeography
262 summarized above.

263

264 **Himalaya**

265 The accretionary fold-thrust belt of the Himalaya consists continent-derived
266 nappes that underlie of ocean-derived accreted units. These accreted rock units play a key
267 role in reconstructing subducted plate paleogeography. Conceptually, accreted rock units
268 fall into two broad types: ocean-derived units consist of Ocean Plate Stratigraphy (OPS),
269 comprising pillow lavas (MORB, OIB, IAT), pelagic oceanic sediments, and foreland
270 basin clastics (53). Continent-derived units consist of Continental Plate Stratigraphy
271 (CPS) that in its simplest form comprises slivers of a basement from an earlier orogenic
272 cycle, an unconformable cover of syn-rift elastic sediments and volcanics, shallow- to
273 deep-marine platform to pelagic passive margin carbonates and occasional clastic series,
274 and foreland basin clastics, although a more complex stratigraphic architecture may form
275 due to climatic or relative sea level variation or a more complex rifting history of the
276 continental margin (31). Key for analyzing the collision and accretion history are the
277 foreland basin clastics: these not only date arrival of the accreted units at a trench, but
278 also allow fingerprinting the nature of the overriding plate through sediment provenance
279 analysis. The moment of accretion of thrust slices is bracketed between the youngest
280 flysch deposits giving a maximum age and, if burial was deep enough, the age of
281 metamorphism (in subduction setting normally of HP-LT type, except during subduction
282 infancy, when HT-HP metamorphic soles may form (54)) of the accreted units, which
283 gives a minimum age (31). Finally, in fold-thrust belts with continuous foreland-
284 propagating thrusting in which almost all subducted lithosphere left its upper crust in the
285 orogen, the youngest age of foreland basin clastics in the higher nappe tends to be similar
286 to the oldest age of foreland basin clastics in the next-lower nappe (as for instance in the
287 Apennines and Hellenides of the Mediterranean region (55)). Conversely, extended
288 periods of non-accretion and wholesale subduction, or subduction erosion removing
289 previously accreted rocks, are revealed by age gaps between foreland basin clastics in
290 adjacent nappes (e.g., in the Japan accretionary prism (53)).

291 The Himalayan fold-thrust belt is commonly divided into four main units, three of
292 which follow the logic outlined above. The highest units, located below the Indus-
293 Yarlung ophiolites is a *mélange* that consists of deformed and in places metamorphosed

294 OPS. These include pillow basalts, cherts that are not older than Triassic in age reflecting
295 the age of opening of the Neotethys ocean (56), and foreland basin clastics in which the
296 youngest recognized ages are ~80 Ma (57). The first-accreted units are dismembered
297 metamorphic sole rocks with ~130 Ma $^{40}\text{Ar}/^{39}\text{Ar}$ cooling ages that provide a minimum
298 age for subduction initiation (58). HP-LT metamorphic OPS units found in the *mélange*
299 below the ophiolites interpreted to have formed during oceanic subduction have ages of
300 100-80 Ma (45).

301 This OPS-derived *mélange* overlies the Tibetan Himalayan nappe. This nappe
302 consists of Paleozoic basement, upper Paleozoic syn-rift clastics and volcanics, a
303 carbonate-dominated passive margin sequence that continues into the Cenozoic (59), and
304 Paleocene to lower Eocene foreland basin clastics whose age estimates range from ~61-
305 54 Ma (18, 19, 60). Metamorphic ages of (U)HP-metamorphic, deeply underthrust
306 equivalents of the Tibetan Himalaya reveal ages suggesting that burial was underway by
307 57 Ma (45). These records provide evidence that continental lithosphere on the Indian
308 plate arrived in a subduction zone by ~60 Ma or shortly thereafter.

309 The Tibetan Himalayan nappes overlie crystalline rocks of the Greater Himalaya.
310 These Greater Himalayan rocks are atypical for accretionary fold-thrust belts in their
311 metamorphic grade as well as their stratigraphy. They consist of Paleozoic pre-
312 Himalayan crystalline basement and sediments that were metamorphosed in Cenozoic
313 times under high-grade metamorphic conditions, up to partial melting, and intruded by
314 leucogranites (8, 61-63). These rocks underwent prograde metamorphism from ~50 Ma
315 onward showing they have been part of the orogen since at least early Eocene time (61,
316 64). The Greater Himalayan sequence is separated from the overlying Tethyan
317 Himalayan sequence by the South Tibetan Detachment (STD), a normal fault that has
318 been active in latest Oligocene to middle Miocene time (61) and that represents a tectonic
319 omission (62) (Fig. 6). No Mesozoic stratigraphy or Cenozoic foreland basin clastic
320 sequences are known from the Greater Himalaya (8, 63). These may either have been cut
321 out by the South Tibetan detachment, which would make the Greater Himalaya a separate
322 nappe derived from crust that was paleogeographically to the south of the Tibetan
323 Himalaya and that underthrust below the Tethyan Himalaya in the early Eocene, or it

324 formed the original stratigraphic underpinnings of the Tethyan Himalaya making them
325 part of the same nappe.

326 The base of the Greater Himalaya is the Main Central Thrust (MCT) a ductile
327 shearzone with a downward decreasing metamorphic grade, signalling syn-exhumation
328 activity, that reveals ages of latest Oligocene to middle Miocene (~26-13 Ma) activity
329 coeval with the South Tibetan Detachment (61, 62). The coeval activity of the MCT and
330 STD is commonly interpreted to reflect extrusion of a mid-crustal part of the orogen (65)
331 that slowly heated up following burial since the Eocene (61). During Miocene extrusion,
332 the Greater Himalayan crystalline rocks were emplaced onto the Lesser Himalayan
333 sequence that contain Lower Miocene foreland basin clastics (see below) and were
334 accreted to the orogen afterwards. There is no geological record of fault zones of Eocene
335 to Miocene age between the Greater and Lesser Himalaya, and the MCT does not appear
336 to reactivate an such a structure (23).

337 The Lesser Himalaya consists of a Paleozoic and older, low-grade
338 metasedimentary, and discontinuous Cretaceous to Paleocene clastic sedimentary rocks,
339 in places overlain by Eocene and Miocene foreland basin clastics (60). Upper Cretaceous
340 to Eocene clastic sedimentary rocks become more prominent towards the west, in
341 Pakistan, where Eocene and younger foreland basin clastics are also found on the
342 undeformed Indian continent (33, 66, 67). The provenance of Upper Cretaceous and
343 Eocene foreland basin clastics in the Lesser Himalayas and on the NW Indian continent
344 reveal erosion of Indian margin rocks and ophiolites that signal Eocene or older
345 obduction, and is commonly interpreted to reflect collision recorded in the Tethyan
346 Himalaya to the north (33, 60, 66, 67). However, the western margin of India was also
347 the locus of orogenesis due to ophiolite emplacement, in a Late Cretaceous and an
348 Eocene phase, but this obduction was governed by convergence between the Indian and
349 Arabian plates and the collision of the Kabul microcontinent with west India (68, 69). So
350 far, the sediment provenance studies have not identified whether the west and north
351 Indian margin have distinctly different signatures presenting an unresolved challenge in
352 interpreting sediment provenance (11). Duplexing of the Lesser Himalayan rocks

353 occurred in the last ~15-13 Ma and accounted for hundreds of kilometers of shortening
354 that is similar to contemporaneous Indian plate consumption (42, 70).

355 The structure of the Himalaya summarized above show an overall foreland
356 propagating fold-thrust belt, but with a clear omission of accretion between the Eocene
357 (Tibetan and Greater Himalaya) and Miocene (Lesser Himalaya). There are two end-
358 member interpretations of this hiatus in accretionary record. Before their Miocene
359 emplacement onto the Lesser Himalaya, the rocks exposed in the Greater Himalaya must
360 have been overlying rocks that have now been transported farther below the orogen and
361 the nature of these rocks is unknown. On the one hand, these rocks may have been the
362 original underlying Indian basement (23, 70) (Fig. 7). In that case, there has been no net
363 convergence between the Greater and Lesser Himalaya between Eocene burial of the
364 former and Miocene burial of the latter. The Eocene-Miocene India-Asia plate boundary
365 must then have been located north of the Himalaya. Of the three models for Indian
366 paleogeography (Fig. 4), only Model A (intra-oceanic arc) could allow for this scenario:
367 in that case, early Eocene burial of the Greater Himalaya follows upon obduction, and
368 activation of the MCT would reflect final collision of the obducted margin with Tibet –
369 but this would require a diachronous Miocene collision age, instead of the proposed 40 ± 5
370 Ma collision ages. All other scenarios require that a subduction plate boundary (intra-
371 continental, or ocean-below continent) existed within the Himalaya. In that case, the
372 Greater Himalayan sequence must have decoupled from its Indian basement sometime
373 after its early Eocene arrival in the orogen, and subsequently formed part of a slowly
374 thickening and heating orogen. In that case, the activation of the MCT displaced the
375 modern Greater Himalayan from a deeper part of the orogen and emplaced it onto the
376 Lesser Himalayan foreland. Such a scenario is typically implied in numerical simulations
377 of Himalayan extrusion and channel flow (71) and interprets the MCT as an out-of-
378 sequence thrust. Importantly any Eo-Oligocene accretionary record and associated thrusts
379 that formed below the Greater Himalayan sequence were then removed from the orogen
380 through subduction erosion upon activation of the MCT (Fig. 7). In Model C and A, this
381 removed part of the orogen consisted of accreted CPS, in Model M (microcontinent), it
382 may also have included OPS.

383

384 Indus-Yarlung ophiolites and Kohistan-Ladakh arc

385 Overlying the accretionary orogen of the Himalaya are a series of ophiolites
386 concentrated in a narrow belt along the northern Himalaya (8) (Figs. 5 and 6). These
387 'Indus-Yarlung' ophiolites are predominantly Early Cretaceous in age (~130-120 Ma),
388 during which time they formed by extension in the forearc above a (presumably
389 incipient) subduction zone (8, 58). In some places also older, Jurassic oceanic crust is
390 found in ophiolites, which may reflect the ocean floor trapped above the subduction zone
391 in which the Cretaceous ophiolites formed (8). In addition, in the western Himalaya, a
392 long-lived intra-oceanic arc sequence (150-50 Ma) that is located between the ophiolites
393 and the continental units of southern Eurasia is known as the Kohistan-Ladakh arc (72).
394 These sequences showed that the accretion of the Himalayan rocks occurred below a
395 forearc that consisted of oceanic lithosphere, which plays a central role in the controversy
396 about Greater Indian paleogeography.

397 The Kohistan-Ladakh arc is overlain by a Cretaceous to Eocene sedimentary
398 sequence and is separated from Tibetan continental rocks by the Shyok Suture (Fig. 5).
399 Convergence across this suture zone has been proposed to be either significant and
400 continuing to Eocene time (27, 28) or minor and pre-dating the late Cretaceous (32), but
401 in any case testifies to the existence of a paleo-subduction zone between the Kohistan-
402 Ladakh arc and Eurasia. The Indus-Yarlung ophiolites are overlain by sediments of the
403 Xigaze forearc basin that form a major syncline with 4-5 km of sediments along 550 km
404 of the subduction zone (73, 74). The oldest sediments are ~130 Ma old and
405 unconformably overlie exhumed oceanic core complexes of the ophiolites and elsewhere
406 interfinger with the ophiolites' pelagic sedimentary cover (75), and the youngest part of
407 the continuous section is ~50 Ma (73, 74). Low-temperature thermochronology revealed
408 that the succession may have been almost twice as thick and suggested that sedimentation
409 and burial may have continued until ~35 Ma (73). The Xigaze forearc has been shortened
410 along the north-dipping Gangdese Thrust, which brought Tibetan rocks over the forearc
411 between ~27 and 23 Ma (76), and the Great Counter thrust that backthrusted the Xigaze
412 forearc over the south Tibetan margin between ~25 and 17 Ma (8) (Fig. 6). Sediment

413 provenance studies of the Xigaze forearc sequence typically depict southern Tibet and its
414 overlying magmatic arc as source (73-75), although others prefer an intra-oceanic arc
415 derivation (26, 27) and there is no known accretionary record of OPS or melange along
416 the strike of the Xigaze forearc basin that may reflect the location of a post-60 Ma
417 paleosubduction zone.

418 The Indus-Yarlung ophiolites have been interpreted as the forearc of the Eurasian
419 plate, whereby they formed by (hyper)-extension of the Tibetan continental lithosphere,
420 occasionally trapping ocean floor that existed before subduction initiation next to the
421 south Tibetan passive margin (77, 78). In this case, the Kohistan-Ladakh arc forms an
422 along-strike, offshore continuation of a contemporaneous arc in Tibet (the Gangdese arc,
423 Fig. 6) and the Shyok suture accommodated only minor convergence that eastwards was
424 accommodated within the Tibetan Plateau (11, 32). This scenario is required by Model C
425 (fully-continental Greater India), and preferred by model M (microcontinent). On the
426 other hand, Model A predicts that the Kohistan-Ladakh arc and Indus-Yarlung ophiolites
427 formed at (or migrated to (8)) equatorial latitudes, far south of the south Tibetan margin,
428 at a separate subduction zone (26-28) from the south Tibetan active margin. This model
429 predicts major convergence across the Shyok Suture, but requires that a long-lived
430 subduction zone is hidden between the Xigaze Basin and the adjacent south Tibetan
431 margin.

432

433 Tibetan Plateau

434 The Tibetan Plateau consists of a series of Gondwana-derived continental fragments and
435 intervening suture zones that amalgamated in Mesozoic time (8, 79). The southernmost of
436 these fragments is the Lhasa Block that accreted to the Tibetan Plateau in early
437 Cretaceous time (8, 79), around the same time as the formation of the south Tibetan
438 ophiolites above a nascent subduction zone to the south of Lhasa (58). Shortening of the
439 Tibetan upper plate above this subduction zone already started in late Cretaceous time,
440 and amounted perhaps already 400 km before initial collision (41, 80, 81) in addition to
441 the 1000-1200 km of post-60 Ma shortening (11, 41). Detailed stratigraphic records
442 reveal that shortening in the plateau may have been pulsed, but there is no evidence of a

443 shortening pulse associated with initial collision around 60 Ma; the recorded pulses may
444 rather reflect changes in Indian subduction rate (21, 81). In Eocene-Oligocene time,
445 shortening was concentrated in the central Tibetan Plateau. Sometime in late Eocene or
446 Oligocene time ($\sim 30 \pm 7$ Ma), Tibetan shortening started to affect the southern margin of
447 the rigid Tarim block to the north of the modern Plateau. To the west of this block,
448 Eurasian lithosphere started to subduct southward, accommodated along the Kashgar-
449 Yecheng transform fault, whereas to the southeast of Tarim, Tibetan crust started to move
450 NE-ward along the Altyn Tagh fault (82). In late Oligocene time, ~ 25 Ma, shortening
451 propagated beyond the Tarim block into the Tien Shan, intensifying at ~ 13 -10 Ma (83).
452 Throughout this history, also NE Tibet underwent outward growth by foreland-
453 propagating thrusting (8, 84).

454 Paradoxically, even though the Tibetan Plateau and Tien Shan underwent ongoing
455 shortening in Oligocene to Early Miocene time, south-central Tibet experienced dynamic
456 subsidence, or even extension. On the southern margin of the Lhasa block, close to the
457 suture zone, formed the 1300 km long Kailas Basin, which forms a southward thickening
458 wedge of >3 km of sediments whose architecture and sedimentology suggests it formed
459 in the hangingwall of a north-dipping normal fault, even though the fault itself is not
460 exposed, perhaps cut out by the Great Counter Thrust (85, 86) (Fig. 6). The stratigraphy
461 in any section of the basin accumulated within only 2-3 Ma, but the timing of basin
462 formation propagates diachronously along-strike, between 26 and 24 Ma in the west, and
463 becoming as young as 18 Ma in the east (86).

464 Upper plate deformation also involved lateral extrusion (40). In the east of the plateau,
465 crust was extruded eastwards already in the Eocene, first accommodated by rotations and
466 thickening in northwest Indochina and later, sometime between ~ 30 and 15 Ma also by
467 motion of entire Indochina along the Red River Fault (87) (Fig. 5). In western Tibet, a
468 similar process may have played a role, although the lack of detailed knowledge of the
469 geology of Afghanistan limits constraints (25). A recent reconstruction of Central Iran
470 (88) pointed out major late Cretaceous to Eocene mobility and E-W convergence across
471 the east Iranian Sistan suture requires that continental fragments of Afghanistan may have
472 undergone major westward displacement (Fig. 5). Restoring such displacement would

473 bring the Aghanistan fragments north of the Kohistan-Ladakh arc and is thus relevant in
474 interpreting its paleolatitudinal history in terms of Greater Indian paleogeography, but
475 awaits future detailed constraints.

476 Around 15-10 Ma, a prominent change in deformation of the Tibetan Plateau occurred,
477 which most famously marks the onset of regional E-W extension in the plateau interior
478 (89, 90) (Fig. 6). Towards the west, this extension is bounded by the Karakoram Fault
479 that accommodated ongoing convergence in the Pamir region (41) (Figs. 5 and 6) and to
480 the east, it is accommodated by E-W shortening in the Longmenshan range, and by a
481 deflection of motion towards the Yunnan region in the southeast, accommodated along
482 major strike-slip faults (3, 90). This motion is prominent today as reflected by GPS
483 measurements. Eastward surface motion components increase from near-zero at the
484 Karakoram Fault eastward to a maximum of ~2 cm/yr on the central plateau (91).
485 Eastward motion components then decrease further to the east due to an increasing
486 southward velocity component in eastern Tibet, as well as E-W shortening in the
487 Longmenshan (90, 91). The extension of the plateau interior and the motion of crust
488 towards the southeast is widely interpreted as driven by excess gravitational potential
489 energy resulting from plateau uplift (3, 47), facilitated by a partially molten middle crust
490 (92). The trigger of extension is thought to reflect middle Miocene uplift of Tibet due to
491 lithospheric delamination (3, 47, 90), or due to Indian continental underthrusting (15).

492 Finally, the Lhasa terrane contains the prominent Gangdese batholith that
493 represents a long-lived volcanic arc (8) (Fig. 6). Arc magmatism in the Lhasa terrane
494 related to Neotethys closure has been active since at least early Cretaceous time and
495 perhaps longer (8). Magmatism of the Gangdese arc since early Cretaceous time
496 contained flareups and periods of reduced activity, but was mostly active until ~45-40
497 Ma, after which there was a lull until 25 Ma (5, 8). During this lull, potassic and
498 ultrapotassic magmatism was active in the Qiangtang terrane, hundreds of kilometers to
499 the north of the Gangdese batholith, after which magmatism resumed in the Lhasa
500 terrane, ultrapotassic or shoshonitic/adakitic in composition (5, 8), associated with
501 economic porphyry copper deposits (6). Since 20 Ma such magmatism also resumed in
502 the Qiangtang and adjacent Songpan Garzi zones of the Tibetan Plateau (5). Interestingly,

503 this Miocene magmatism in the Lhasa terrane migrated eastward, 25-20 Ma in western
504 Tibet but 15-10 Ma in the east, towards the longitude of Bhutan (7). The chemistry of
505 these magmatic rocks is interpreted to be mostly derived from a previously subduction-
506 enriched asthenospheric source that became stirred by the underthrusting continental
507 Indian lithosphere (5-7).

508

509 Discussion

510 Opportunities, 1: Natural laboratory of converging unsubductable lithospheres

511 The kinematic reconstruction constraining of horizontal continental underthrusting of the
512 Indian continent below Tibet identifies (only) the Miocene and younger history of the
513 Tibetan-Himalayan geological history as natural laboratory for the convergence of
514 unsubductable lithospheres. While and extensive analysis of the dynamics of this system
515 is beyond the scope of this paper, several first-order temporal and spatial relationships
516 between horizontal underthrusting and geological evolution are clear and may be used as
517 basis to discern between existing hypotheses, or develop new.

518 Most importantly, the irregular shape of the seismically imaged northern Indian
519 continental margin shows that initial horizontal underthrusting must have been
520 diachronous: the coinciding age estimates from the kinematic restoration of this margin
521 (16) (Fig. 3) and geological estimates of the youngest phase of slab break-off from the
522 Himalaya (17) of ~25 Ma at the Himalayan syntaxes, decreasing to ~13 Ma in at the
523 longitude of Bhutan, may provide means to discern between the effects of horizontal
524 underthrusting and unrelated events. For instance, the re-initiation of magmatism between
525 25 and 8 Ma in the Lhasa terrane follows the same age progression, lending independent
526 support to the interpretation that magmatism resulted from incipient Indian continental
527 lithosphere plowing through and stirring of a previously subduction-enriched
528 asthenosphere (5-7, 93). On the other hand, Miocene magmatism farther north in the
529 Tibetan plateau that started around 20 Ma is located far away from the horizontally
530 underthrusting northern Indian continental margin, and does not show a lateral age
531 progression, making a direct link unlikely.

532 The formation and deposition of the Kailas basin follows the same diachronous trend, but
533 precedes the reconstructed slab break-off by a few Ma (86). The recognition of
534 diachronous initial horizontal underthrusting allows explaining this trend, as well as the
535 apparent paradox of N-S extension in the Kailas Basin of southern Tibet (85, 86) and the
536 coeval ongoing upper plate shortening in the Pamir, along the Altyn Tagh fault, and in
537 NE Tibet (82, 84). The subsidence of the Kailas basin is well explained as the result of
538 negative dynamic topography, or even upper plate extension, caused by the Himalayan
539 slab resisting slab advance, just prior to its detachment (16, 86, 94) (Fig. 8). This
540 resistance only occurs where the slab is still attached, explaining the diachroneity in
541 Kailas Basin formation and its subsequent uplift. But where slab detachment has already
542 occurred, i.e. at the longitude of the Himalayan syntaxes, the Pamir and eastern Tibet,
543 horizontal Indian underthrusting may already have caused enhanced friction to drive the
544 apparently paradoxical simultaneous upper plate shortening and extension (Fig. 8).

545 The reconstructed horizontal Indian underthrusting also sheds light on the long-standing
546 debate on the trigger of E-W extension in Tibet. There is widespread consensus that this
547 extension reflects the gravitational collapse of the Tibetan Plateau (3, 15, 47, 90),
548 whereby as final trigger, lithosphere delamination of south-central Tibet (3, 47, 90) or
549 uplift due to horizontal Indian underthrusting (15) have been suggested. Horizontally
550 underthrust Indian continental lithosphere directly underlies Tibetan crust, and its
551 lithospheric mantle must thus have delaminated prior to the 25 Ma onset of horizontal
552 underthrusting in western and eastern Tibet. In addition, not only the source area below
553 the Tibetan Plateau, but also the ‘sink’ of Middle Miocene and younger crustal motion in
554 the Yunnan region has undergone lithospheric delamination (49). This suggests that the
555 15-10 Ma onset of E-W extension was likely not triggered by delamination. More likely,
556 collapse was driven by the final onset of horizontal underthrusting below the entire
557 plateau following final slab break-off (15). If horizontal underthrusting indeed caused
558 uplift, the easternmost part of the Indian continental promontory north of the eastern
559 syntaxis may have first formed a barrier against plateau collapse, which was only
560 overcome after the entire Tibetan Plateau became horizontally underthrust by India since
561 middle Miocene time.

562 Also middle Miocene changes in the Himalaya may be studied in context of the transition
563 from subduction to horizontal underthrusting. Webb et al. (17) already interpreted syntaxis
564 formation and Himalayan oroclinal bending as result of the change to horizontal
565 underthrusting. Also the transition from extrusion of the Greater Himalayan crystalline
566 rocks along the STD and MCT, to duplexing of the Lesser Himalayan nappes appears to
567 coincide with the transition to horizontal underthrusting, but future analyses may test
568 whether there was diachroneity in these processes. The coincidence of intraplate
569 deformation events, e.g. in the Tien Shan with the onset of horizontal underthrusting in
570 western Tibet around 25, and along the entire Tibetan margin around 13 Ma, may suggest
571 a causal relationship linking convergence between unsubductable lithosphere to intraplate
572 deformation. On the other hand, the shortening in the Tien Shan may also be a natural
573 northward progression of intraplate deformation that had long been ongoing in the
574 Tibetan plateau. Future numerical experiments may test such dynamic hypotheses built
575 on the Miocene Tibetan-Himalayan natural laboratory for the convergence of
576 unsubductable lithosphere.

577

578 [Opportunities, 2: Improving methodology to unlock the post-collisional](#) 579 [subduction laboratory](#)

580 The ongoing controversy of Greater Indian paleogeography currently hampers using the
581 interval between initial collision, around 60 Ma, and the 25-13 Ma of horizontal Indian
582 underthrusting as a conclusive natural laboratory for post-collisional subduction.

583 Regardless of which of scenarios of Model C, A, or M will turn out to be correct, if any,
584 this natural laboratory holds great promise. Models C and A so far offer no explanation
585 for why there was a transition from subduction to horizontal underthrusting, or what
586 caused the diachroneity of that transition, but if these scenarios are correct, that
587 explanation must provide a unique constraint on the subductability of continental
588 lithosphere. Moreover, Models C and A predict that continental subduction is also
589 possible without preservation of upper crustal units, or with large-scale subsequent
590 removal of accreted continental crust through subduction erosion. If these models are
591 correct, it is thus possible that paleogeographic reconstructions strongly underestimate

592 the paleogeographic area occupied by continental lithosphere. In fact, if large portions of
593 continental lithosphere can subduct without leaving a geological record, accreted
594 geological records such as in the Tibetan Himalaya cannot provide conclusive constraints
595 on initial collision, but only give a minimum age (31). Finally, model C (since 60 Ma)
596 and model A (since 40 ± 5 Ma) would provide the opportunity to calibrate magmatic
597 responses to continental subduction.

598 The subduction history of model M is entirely on par with current geodynamic
599 paradigms, with a short-lived, late Paleocene to early Eocene phase of microcontinental
600 lower crust and mantle lithosphere subduction combined with upper crustal accretion that
601 is well-documented elsewhere (55) and found plausible in numerical experiments (95). In
602 model M, upper crustal nappes of all subducted or horizontally underthrust continental
603 lithosphere still remain in the Himalayan orogen (11). The transition from subduction to
604 horizontal underthrusting in model M is simply caused by the change from oceanic to
605 continental subduction. But model M invokes that the anomalous magmatic history of
606 Tibet between 45 and the 25 Ma onset of horizontal underthrusting occurred during
607 oceanic (perhaps flat slab (11, 86)) subduction and would thus allow calibrating possible
608 magmatic arc expressions of anomalous oceanic subduction.

609 The three models provide strongly different boundary conditions and have far-reaching
610 consequences for the analysis of the dynamic drivers of upper and intraplate deformation,
611 the causes of rapid plate motion changes of India, or the causes and paleogeographic
612 context of terrestrial biota exchange and radiation. It is therefore important to attempt at
613 breaking through the impasse in Greater Indian paleogeography reconstruction. I will
614 attempt at briefly identifying where opportunities may lie to achieve this.

615 The only quantitative constraint on paleogeographic position comes from paleomagnetic
616 data providing paleolatitudinal control. Paleomagnetic analyses on rocks derived from
617 Greater India such as the Tibetan Himalayan sequence, of ophiolites and intra-oceanic
618 arcs and their cover, and of the Lhasa terrane of southern Tibet in principle allows
619 discerning between Model C, A, and M. But each of these models has been defended and
620 and challenged based on paleomagnetic data (27, 29, 34-37). So are paleomagnetic data
621 inconclusive? Rowley (34) recently pointed out that the widely used method to compare

622 paleomagnetic study means ('paleopoles') with apparent polar wander paths that provide
623 the global reference against which these data are compared and that are based on
624 averages of study means, is indeed barely conclusive. The paleopoles underlying APWPs
625 are scattered by $\sim 20^\circ$ around the mean, and Rowley (34) argued that individual
626 paleopoles cannot constrain paleolatitude at a higher resolution. Vaes et al. (96),
627 however, recently analyzed the source of this scatter, and showed that alongside common
628 paleomagnetic artifacts such as undersampling of paleosecular variation, and inclination
629 shallowing in sediments, scatter is mostly caused by the degree to which paleosecular
630 variation is averaged: scatter is a function of the number of paleomagnetic datapoints
631 used to determine a paleopole. And because this number is arbitrary, the statistical
632 properties of APWPs calculated from paleopoles are arbitrary. Vaes et al. (96) provided a
633 way forward in which paleopoles are compared to a reference curve that is also calculated
634 from paleomagnetic readings rather than paleopoles, and developed a comparison metric
635 that demonstrates a paleolatitudinal difference or vertical axis rotation with 95%
636 confidence. This would provide a means to compare datasets of unequal magnitude and
637 propagate uncertainties, and may provide a more conclusive, quantitative, and robust
638 paleomagnetic analysis that may discern between the Greater Indian paleogeography
639 models.

640 Models C, A, and M each invoke that a plate boundary must have existed south of the
641 Tibetan Plateau between the Paleocene to Early Eocene accretion of the Tibetan and
642 Greater Himalayan units in the orogen, and the accretion of the Miocene Lesser
643 Himalayan units. If this plate boundary was located in the Himalayas during all or some
644 of the period between 60 and 25/13 Ma, as currently required by all three scenarios, there
645 may be no record due to out-of-sequence thrusting along the MCT removing the pre-
646 Miocene underpinnings (Fig. 7). But this refocuses the attention on the process of
647 extrusion and channel flow, this time not to explain the presence of the Greater
648 Himalayan rocks in the orogen, but to explain the absence of its pre-Miocene
649 underpinnings. In addition, Models C and A require that a subduction plate boundary was
650 present between the Xigaze forearc and underlying ophiolites, and the Lhasa terrane (8).
651 Detailed mapping, or identifying structures that could explain the lack of a record such as

652 I argue for the MCT (Fig. 7), may establish whether, when, and where such a subduction
653 zone may have existed.

654 Also sediment provenance studies have been used to argue for and against Models C, A,
655 and M. Part of this may underlie the qualitative nature of comparing e.g. detrital
656 geochronology peaks between the sedimentary record of a sink and a suspected source
657 area, and recently developed quantitative approaches that identify the likelihood of the
658 contribution of a given source area to a sediment may advance the discussion (97). In this
659 analysis, the range of possible source areas for sediments, particularly for Eocene
660 stratigraphic records in the NW Lesser Himalaya and the Pakistani foreland should
661 include not only the Himalaya-Kohistan-Ladakh-Tibetan orogen at the India-Asia plate
662 boundary, but also the Sulaiman-Kabul Block orogen and associated ophiolites that
663 formed independently at the India-Arabia plate boundary (68, 69) (Fig. 4).

664 Seismic tomographic records of subducted slabs are useful in identifying regions of
665 paleo-subduction (38, 39), although global correlations suggest that the lower mantle
666 hosts slabs of the last ~250 Ma (50). Analysis of mantle structure should hence be done
667 in context of Mesozoic and Cenozoic subduction history and uncertainties therein (16)
668 (Fig. 2). Nonetheless, a recent seismological study of a slab below Kamchatka was able
669 to identify thick crust, on the order of 20 km, in a lower mantle slab (98). Once a slab can
670 be firmly tied to lithosphere that subducted after initial collision, such as the overturned
671 Himalayan slab that straddles the transition zone (13, 38), such seismological analyses
672 may provide novel constraints on their composition and crustal nature.

673 In summary, on the one hand, the current controversy on Indian paleogeography
674 stemming from the inability of geological and geophysical techniques to conclusively
675 identify between vastly different paleogeographic scenarios, stands in the way of using
676 the India-Asia collision zone to calibrate the geological and dynamic responses to post-
677 collisional subduction. On the other hand, this controversy provides the opportunity (and
678 requires) to question and improve geological methodology to constrain paleogeography,
679 including orogen structure, sediment provenance analysis, and paleomagnetism. Solving
680 those issues have impact far beyond the analysis of the India-Asia collision history.

681

682 Conclusions

683 Seismological images reveal that 400-800 km of Indian continental lithosphere is
684 currently horizontally underthrust below Tibet. Using plate reconstructions that
685 incorporate Tibetan shortening predict that the onset of horizontal underthrusting started
686 around 25 Ma around the Himalayan syntaxes, gradually younging to 13 Ma at the
687 longitude of Bhutan. This reconstruction coincides with independent estimates of
688 diachronous slab break-off in the Himalaya, and identifies the Miocene history of Tibet
689 as a natural laboratory for convergence of unsubductable lithospheres. This time period
690 was marked by major changes in accretionary style in the Himalayas, including the
691 extrusion of the Greater Himalayan crystalline rocks and the transition to Lesser
692 Himalayan duplexing, but also by the onset of E-W extension and collapse of the Tibetan
693 Plateau, and upper plate shortening reaching as far north as the Tien Shan. Also marked
694 changes in magmatism in southern Tibet, and associated economic mineralizations
695 spatially and temporally correlate with the reconstructed inception horizontal
696 underthrusting. These processes may provide key ingredients of the natural laboratory for
697 convergence of unsubductable lithosphere. Importantly, lithospheric delamination of
698 Tibet, often cited as potential trigger for Miocene Tibetan uplift and collapse, must
699 instead have occurred prior to horizontal Indian underthrusting, hence before the
700 Miocene.

701 Between initial collision recorded in the Himalaya at 60 Ma and the onset of horizontal
702 Indian underthrusting, thousands of kilometers of subduction consumed Indian plate
703 lithosphere. I discuss three end-member scenarios that invoke that all or part of this
704 lithosphere was continental, challenging geodynamic and paleogeographic reconstruction
705 paradigms, or that most of this lithosphere was oceanic, challenging magmatic and
706 orogenic architecture paradigms. But an impasse is reached because each of these
707 reconstructions is argued for and against based on the same datatypes. I identify
708 opportunities for methodological advances in fields including paleomagnetism, sediment
709 provenance analysis, and seismology to overcome this impasse, unlocking the 60-25/13
710 Ma interval of Tibetan and Himalayan evolution as natural laboratory for typical

711 geological responses for a-typical post-collisional subduction, or for a-typical geological
712 responses to typical oceanic subduction.

713

714 Acknowledgements

715 I thank my friends and collaborators Wim Spakman, Pete Lippert, Carl Guilmette,
716 Wentao Huang, Shihu Li, Zhenyu Li, Guillaume Dupont-Nivet, Abdul Qayyum, Paul
717 Kapp, Thomas Schouten, Licheng Cao, and Eldert Advokaat for the many discussions
718 that inspired me to write this paper.

719

720 Funding

721 This work was supported by Netherlands Organization for Scientific Research Vici grant
722 865.17.001.

723

724 Author contributions

725 DJJvH is the sole author of this paper, performed analyses, and drafted figures.

726

727 **Figure captions**

728

729 **Fig. 1.** Reconstructed India-Asia convergence (21), which, when corrected for Tibetan
730 shortening (11) predicts Indian plate subduction/underthrusting for the last 60 Ma. The
731 amount of post-collisional subduction is a function of initial collision age recorded in the
732 Himalaya (60-55 Ma) (18, 19, 45) and the width of horizontally underthrust India, which
733 varies along-strike from 400-800 km (at the longitude of the reference location, this width
734 is ~400 km, Fig. 2).

735

736 **Fig. 2.** Seismic tomographic images taken from the UU-P07 tomography model (50, 99).
737 **A)** Vertical section from the Indian Ocean to Central Asia (drawn using the Hades
738 Underworld Explorer, www.atlas-of-the-underworld.org). Deep, flat-lying slabs relate to
739 Mesozoic Paleotethys and Mesotethys subduction during the amalgamation of Tibetan
740 terranes (16). The India slab contains the bulk of Neotethys lithosphere that subducted
741 northward below the Lhasa terrane, whereas the northward subducted but overturned
742 Himalaya slab contains subducted Greater Indian lithosphere (11, 13, 16, 38, 39).
743 Horizontally underthrust Indian continental lithosphere protrudes northward from the
744 Main Frontal Thrust over a distance of 400-800 km, varying along-strike (9-12, 16). **B).**
745 Horizontal cross-section at 110 km depth through the UU-P07 tomography model,
746 overlain by outlines of modern geology and geography. The yellow dotted line depicts
747 the outline of the northern margin of horizontally underthrust Indian continent below
748 Tibet, protruding ~800 km northward north of the Himalayan syntaxes, decreasing to
749 ~400 km towards ~90°E (9, 11, 12)

750

751 **Fig. 3.** Reconstructions of the diachronous onset of horizontal Indian underthrusting at
752 **(A)** 28 Ma; **(B)** 15 Ma, and **(C)** the Present Day, using the outline of horizontally
753 underthrust continental lithosphere of India shown in Figure tomography, using the

754 kinematic reconstruction of Tibet and the Himalaya of reference (11), and India-Asia
755 convergence following reference (21).

756

757 **Fig. 4.** Paleogeographic maps at the time of initial collision (~60 Ma (18, 19, 45)) and in
758 Gondwana fits at 155, corresponding to the timing of continental breakup in the Argo
759 Abyssal Plain between Northwest Australia and the conceptual Argoland continent (51),
760 for three end-member models discussed in the text. Models are placed in the
761 paleomagnetic reference frame of reference (100). **A)** Model C, with a fully continental
762 Greater India (19, 23, 24, 40); **B)** Model A, in which initial collision occurred with an
763 intra-oceanic subduction zone around the equator. The size of continental Greater India is
764 here constructed with a 40 Ma closure age of the remaining oceanic lithosphere (8, 25-28,
765 52); Model C), in which 60 Ma collision occurs between a microcontinent that broke off
766 Northern India in the Cretaceous, opening a Greater India Basin in its wake (11, 29).
767 AAP = Argo Abyssal Plain; CRFZ = Cape Range Fracture Zone; KLA = Kohistan-
768 Ladakh Arc; PAO = Pakistan Ophiolites; TH = Tibetan Himalaya; WBB = West Burma
769 Block; WFZ = Wallaby Fracture Zone; XFB = Xigaze Forearc Basin.

770

771 **Fig. 5.** Tectonic map of the India-Asia collision zone, modified after reference (11). Mct
772 = Main Central Thrust; mft = Main Frontal Thrust; RRF = Red River Fault; std = South
773 Tibetan Detachment.

774

775 **Fig. 6. A)** Tectonic map of the Himalaya and Tibet, simplified after references (58, 85,
776 86). **B)** Schematic cross section through the Himalayas and southern Tibet, modified
777 from reference (8). ATF = Altyn Tagh Fault; GCT = Great Counter Thrust; GT =
778 Gangdese Thrust; IYSZ = Indus-Yarlung Suture Zone; KF = Karakoram Fault; MCT =
779 Main Central Thrust; MFT = Main Frontal Thrust; MHT = Main Himalayan Thrust; STD
780 = South Tibetan Detachment.

781

782 **Fig. 7.** Conceptual evolution of Himalayan architecture if **A)** all Eocene-early Miocene
783 India-Asia convergence is accommodated to the north of the Himalaya. In this case, the
784 MCT can have formed when the GH rocks decoupled from their original Indian lower
785 crustal and lithospheric underpinnings, or **B)**, all or part of the Eocene-early Miocene
786 India-Asia convergence is accommodated within the Himalaya. In this case, the MCT is
787 an out-of-sequence thrust that formed within the early Miocene Himalayan fold-thrust
788 belt and Eocene-Miocene units that may have accreted below the Greater Himalaya have
789 been removed by subduction erosion.

790

791 **Fig. 8.** Cartoon illustrating geometrical relationships between diachronous slab
792 detachment and onset of horizontal Indian continental lithospheric underthrusting below
793 Tibet between 25 and 13 Ma, and geological expressions in the Tibetan Plateau.

794

795 References

796

797

798

799

800

801

802

803

804

805

806

807

808

809

810

811

812

813

814

815

816

817

818

819

820

821

822

823

824

825

826

827

828

829

830

831

832

833

834

835

836

837

838

1. Vlaar, N, Wortel, M. Lithospheric aging, instability and subduction. *Tectonophysics*. 1976; **32**(3-4): 331-51.
2. Cloos, M. Lithospheric buoyancy and collisional orogenesis: Subduction of oceanic plateaus, continental margins, island arcs, spreading ridges, and seamounts. *Geological Society of America Bulletin*. 1993; **105**(6): 715-37.
3. Molnar, P, England, P, Martinod, J. Mantle dynamics, uplift of the Tibetan Plateau, and the Indian monsoon. *Reviews of Geophysics*. 1993; **31**(4): 357-96.
4. Su, T, Spicer, RA, Li, S-H, *et al*. Uplift, climate and biotic changes at the Eocene–Oligocene transition in south-eastern Tibet. *National Science Review*. 2019; **6**(3): 495-504.
5. Xia, L, Li, X, Ma, Z, *et al*. Cenozoic volcanism and tectonic evolution of the Tibetan plateau. *Gondwana Research*. 2011; **19**(4): 850-66.
6. Sun, X, Lu, Y, Li, Q, *et al*. A downgoing Indian lithosphere control on along-strike variability of porphyry mineralization in the Gangdese belt of southern Tibet. *Economic Geology*. 2021; **116**(1): 29-46.
7. Nomade, S, Renne, PR, Mo, X, *et al*. Miocene volcanism in the Lhasa block, Tibet: spatial trends and geodynamic implications. *Earth and Planetary Science Letters*. 2004; **221**(1-4): 227-43.
8. Kapp, P, DeCelles, PG. Mesozoic–Cenozoic geological evolution of the Himalayan–Tibetan orogen and working tectonic hypotheses. *American Journal of Science*. 2019; **319**(3): 159-254.
9. Li, J, Song, X. Tearing of Indian mantle lithosphere from high-resolution seismic images and its implications for lithosphere coupling in southern Tibet. *Proceedings of the National Academy of Sciences*. 2018; **115**(33): 8296-300.
10. Chen, M, Niu, F, Tromp, J, *et al*. Lithospheric foundering and underthrusting imaged beneath Tibet. *Nature communications*. 2017; **8**(1): 1-10.
11. van Hinsbergen, DJJ, Lippert, PC, Li, S, *et al*. Reconstructing Greater India: Paleogeographic, kinematic, and geodynamic perspectives. *Tectonophysics*. 2019; **760**: 69-94.
12. Agius, MR, Lebedev, S. Tibetan and Indian lithospheres in the upper mantle beneath Tibet: Evidence from broadband surface-wave dispersion. *Geochemistry, Geophysics, Geosystems*. 2013; **14**(10): 4260-81.
13. Replumaz, A, Negrodo, AM, Villaseñor, A, *et al*. Indian continental subduction and slab break-off during Tertiary collision. *Terra Nova*. 2010; **22**: 290-6.
14. Nabelek, J, Hetenyi, G, Vergne, J, *et al*. Underplating in the Himalaya–Tibet collision zone revealed by the Hi-CLIMB experiment. *Science*. 2009; **325**(5946): 1371-4.
15. Styron, R, Taylor, M, Sundell, K. Accelerated extension of Tibet linked to the northward underthrusting of Indian crust. *Nature Geoscience*. 2015; **8**(2): 131-4.
16. Qayyum, A, Lom, N, Advokaat, EL, *et al*. Subduction and slab detachment under moving trenches during ongoing India–Asia convergence. *Earth and Space Science Open Archive*. 2022: 45.

- 839 17. Webb, AAG, Guo, H, Clift, PD, *et al.* The Himalaya in 3D: Slab dynamics
840 controlled mountain building and monsoon intensification. *Lithosphere*. 2017.
- 841 18. An, W, Hu, X, Garzanti, E, *et al.* New precise dating of the India-Asia collision in
842 the Tibetan Himalaya at 61 Ma. *Geophysical Research Letters*. 2021; **48**(3):
843 e2020GL090641.
- 844 19. Hu, X, Garzanti, E, Wang, J, *et al.* The timing of India-Asia collision onset –
845 Facts, theories, controversies. *Earth-Science Reviews*. 2016; **160**: 264-99.
- 846 20. van Hinsbergen, DJJ, Steinberger, B, Doubrovine, PV, *et al.* Acceleration and
847 deceleration of India-Asia convergence since the Cretaceous: Roles of mantle plumes and
848 continental collision. *Journal of Geophysical Research*. 2011; **116**(B6).
- 849 21. DeMets, C, Merkouriev, S. Detailed reconstructions of India–Somalia Plate
850 motion, 60 Ma to present: implications for Somalia Plate absolute motion and India–
851 Eurasia Plate motion. *Geophysical Journal International*. 2021; **227**(3): 1730-67.
- 852 22. van Hunen, J, Allen, MB. Continental collision and slab break-off: A comparison
853 of 3-D numerical models with observations. *Earth and Planetary Science Letters*. 2011;
854 **302**(1-2): 27-37.
- 855 23. Searle, MP. Timing of subduction initiation, arc formation, ophiolite obduction
856 and India–Asia collision in the Himalaya. *Geological Society, London, Special
857 Publications*. 2018; **483**: SP483. 8.
- 858 24. Ingalls, M, Rowley, DB, Currie, B, *et al.* Large-scale subduction of continental
859 crust implied by India–Asia mass-balance calculation. *Nature Geoscience*. 2016; **9**(11):
860 848-53.
- 861 25. Tapponnier, P, Mattauer, M, Proust, F, *et al.* Mesozoic ophiolites, sutures, and
862 large-scale tectonic movements in Afghanistan. *Earth and Planetary Science Letters*.
863 1981; **52**(2): 355-71.
- 864 26. Aitchison, JC, Ali, JR, Davis, AM. When and where did India and Asia collide?
865 *Journal of Geophysical Research*. 2007; **112**(B5).
- 866 27. Martin, CR, Jagoutz, O, Upadhyay, R, *et al.* Paleocene latitude of the Kohistan–
867 Ladakh arc indicates multistage India–Eurasia collision. *Proceedings of the National
868 Academy of Sciences*. 2020; **117**(47): 29487-94.
- 869 28. Jagoutz, O, Royden, L, Holt, AF, *et al.* Anomalously fast convergence of India
870 and Eurasia caused by double subduction. *Nature Geoscience*. 2015; **8**(6): 475-8.
- 871 29. van Hinsbergen, DJJ, Lippert, PC, Dupont-Nivet, G, *et al.* Greater India Basin
872 hypothesis and a two-stage Cenozoic collision between India and Asia. *Proc Natl Acad
873 Sci U S A*. 2012; **109**(20): 7659-64.
- 874 30. Cawood, PA, Kröner, A, Collins, WJ, *et al.* Accretionary orogens through Earth
875 history. *Geological Society, London, Special Publications*. 2009; **318**(1): 1-36.
- 876 31. van Hinsbergen, DJJ, Schouten, TLA. Deciphering paleogeography from orogenic
877 architecture: constructing orogens in a future supercontinent as thought experiment.
878 *American Journal of Science*. 2021; **321**: 955-1031.
- 879 32. Borneman, NL, Hodges, KV, Van Soest, MC, *et al.* Age and structure of the
880 Shyok suture in the Ladakh region of northwestern India: implications for slip on the
881 Karakoram fault system. *Tectonics*. 2015; **34**(10): 2011-33.
- 882 33. Ding, L, Qasim, M, Jadoon, IAK, *et al.* The India–Asia collision in north
883 Pakistan: Insight from the U–Pb detrital zircon provenance of Cenozoic foreland basin.
884 *Earth and Planetary Science Letters*. 2016; **455**: 49-61.

- 885 34. Rowley, DB. Comparing Paleomagnetic Study Means with Apparent Wander
886 Paths: A Case Study and Paleomagnetic Test of the Greater India versus Greater Indian
887 Basin Hypotheses. *Tectonics*. 2019; **38**: 722-40.
- 888 35. Yuan, J, Yang, Z, Deng, C, *et al.* Rapid drift of the Tethyan Himalaya terrane
889 before two-stage India-Asia collision. *National Science Review*. 2021; **8**(7): nwaal73.
- 890 36. Jadoon, UF, Huang, B, Shah, SA, *et al.* Multi-stage India-Asia collision:
891 Paleomagnetic constraints from Hazara-Kashmir syntaxis in the western Himalaya. *GSA*
892 *Bulletin*. 2021.
- 893 37. Yang, T, Jin, J, Bian, W, *et al.* Precollisional latitude of the Northern Tethyan
894 Himalaya from the Paleocene redbeds and its implication for greater India and the India-
895 Asia collision. *Journal of Geophysical Research: Solid Earth*. 2019; **124**(11): 10777-98.
- 896 38. Parsons, AJ, Hosseini, K, Palin, R, *et al.* Geological, geophysical and plate
897 kinematic constraints for models of the India-Asia collision and the post-Triassic central
898 Tethys oceans. *Earth-Science Reviews*. 2020: 103084.
- 899 39. Van der Voo, R, Spakman, W, Bijwaard, H. Tethyan subducted slabs under India.
900 *Earth and Planetary Science Letters*. 1999; **171**(1): 7-20.
- 901 40. Replumaz, A, Tapponnier, P. Reconstruction of the deformed collision zone
902 Between India and Asia by backward motion of lithospheric blocks. *Journal of*
903 *Geophysical Research: Solid Earth*. 2003; **108**(B6).
- 904 41. van Hinsbergen, DJJ, Kapp, P, Dupont-Nivet, G, *et al.* Restoration of Cenozoic
905 deformation in Asia and the size of Greater India. *Tectonics*. 2011; **30**(5): n/a-n/a.
- 906 42. Long, S, McQuarrie, N, Tobgay, T, *et al.* Geometry and crustal shortening of the
907 Himalayan fold-thrust belt, eastern and central Bhutan. *Geological Society of America*
908 *Bulletin*. 2011; **123**(7-8): 1427-47.
- 909 43. Patriat, P, Achache, J. India-Eurasia collision chronology has implications for
910 crustal shortening and driving mechanism of plates. *Nature*. 1984; **311**: 615-21.
- 911 44. Hu, X, Garzanti, E, Moore, T, *et al.* Direct stratigraphic dating of India-Asia
912 collision onset at the Selandian (middle Paleocene, 59 ± 1 Ma). *Geology*. 2015; **43**(10):
913 859-62.
- 914 45. Guillot, S, Mahéo, G, de Sigoyer, J, *et al.* Tethyan and Indian subduction viewed
915 from the Himalayan high- to ultrahigh-pressure metamorphic rocks. *Tectonophysics*.
916 2008; **451**(1-4): 225-41.
- 917 46. McKenzie, D, Priestley, K. The influence of lithospheric thickness variations on
918 continental evolution. *Lithos*. 2008; **102**(1-2): 1-11.
- 919 47. England, P, Houseman, G. Extension during continental convergence, with
920 application to the Tibetan Plateau. *Journal of Geophysical Research: Solid Earth*. 1989;
921 **94**(B12): 17561-79.
- 922 48. Replumaz, A, Guillot, S, Villaseñor, A, *et al.* Amount of Asian lithospheric
923 mantle subducted during the India/Asia collision. *Gondwana Research*. 2013; **24**(3-4):
924 936-45.
- 925 49. Feng, J, Yao, H, Chen, L, *et al.* Massive lithospheric delamination in southeastern
926 Tibet facilitating continental extrusion. *National Science Review*. 2021.
- 927 50. van der Meer, DG, van Hinsbergen, DJJ, Spakman, W. Atlas of the underworld:
928 Slab remnants in the mantle, their sinking history, and a new outlook on lower mantle
929 viscosity. *Tectonophysics*. 2018; **723**: 309-448.

- 930 51. Gibbons, AD, Barckhausen, U, van den Bogaard, P, *et al.* Constraining the
931 Jurassic extent of Greater India: Tectonic evolution of the West Australian margin.
932 *Geochemistry Geophysics Geosystems*. 2012; **13**.
- 933 52. Westerweel, J, Roperch, P, Licht, A, *et al.* Burma Terrane part of the Trans-
934 Tethyan arc during collision with India according to palaeomagnetic data. *Nature*
935 *Geoscience*. 2019; **12**(10): 863-8.
- 936 53. Isozaki, Y, Maruyama, S, Furuoka, F. Accreted oceanic materials in Japan.
937 *Tectonophysics*. 1990; **181**(1-4): 179-205.
- 938 54. Agard, P, Yamato, P, Soret, M, *et al.* Plate interface rheological switches during
939 subduction infancy: Control on slab penetration and metamorphic sole formation. *Earth*
940 *and Planetary Science Letters*. 2016; **451**: 208-20.
- 941 55. van Hinsbergen, DJJ, Torsvik, T, Schmid, SM, *et al.* Orogenic architecture of the
942 Mediterranean region and kinematic reconstruction of its tectonic evolution since the
943 Triassic. *Gondwana Research*. 2020; **81**: 79-229.
- 944 56. Ziabrev, SV, Aitchison, JC, Abrajevitch, AV, *et al.* Bainang Terrane, Yarlung–
945 Tsangpo suture, southern Tibet (Xizang, China): a record of intra-Neotethyan
946 subduction–accretion processes preserved on the roof of the world. *Journal of the*
947 *Geological Society*. 2004; **161**(3): 523-39.
- 948 57. An, W, Hu, X, Garzanti, E. Discovery of Upper Cretaceous Neo-Tethyan trench
949 deposits in south Tibet (Luogangcuo Formation). *Lithosphere*. 2018; **10**(3): 446-59.
- 950 58. Guilmette, C, Hébert, R, Wang, C, *et al.* Geochemistry and geochronology of the
951 metamorphic sole underlying the Xigaze Ophiolite, Yarlung Zangbo Suture Zone, South
952 Tibet. *Lithos*. 2009; **112**(1-2): 149-62.
- 953 59. Garzanti, E. Stratigraphy and sedimentary history of the Nepal Tethys Himalaya
954 passive margin. *Journal of Asian Earth Sciences*. 1999; **17**(5-6): 805-27.
- 955 60. DeCelles, PG, Kapp, P, Gehrels, GE, *et al.* Paleocene-Eocene foreland basin
956 evolution in the Himalaya of southern Tibet and Nepal: Implications for the age of initial
957 India-Asia collision. *Tectonics*. 2014; **33**(5): 824-49.
- 958 61. Carosi, R, Montomoli, C, Iaccarino, S. 20 years of geological mapping of the
959 metamorphic core across Central and Eastern Himalayas. *Earth-Science Reviews*. 2018;
960 **177**: 124-38.
- 961 62. Hodges, KV. Tectonics of the Himalaya and southern Tibet from two
962 perspectives. *Geological Society of America Bulletin*. 2000; **112**(3): 324-50.
- 963 63. Yin, A. Cenozoic tectonic evolution of the Himalayan orogen as constrained by
964 along-strike variation of structural geometry, exhumation history, and foreland
965 sedimentation. *Earth-Science Reviews*. 2006; **76**(1-2): 1-131.
- 966 64. Smit, MA, Hacker, BR, Lee, J. Tibetan garnet records early Eocene initiation of
967 thickening in the Himalaya. *Geology*. 2014; **42**(7): 591-4.
- 968 65. Grujic, D, Casey, M, Davidson, C, *et al.* Ductile extrusion of the Higher
969 Himalayan Crystalline in Bhutan: evidence from quartz microfabrics. *Tectonophysics*.
970 1996; **260**(1-3): 21-43.
- 971 66. Khan, I, Clyde, W. Lower Paleogene Tectonostratigraphy of Balochistan:
972 Evidence for Time-Transgressive Late Paleocene-Early Eocene Uplift. *Geosciences*.
973 2013; **3**(4): 466-501.

- 974 67. Qasim, M, Ahmad, J, Ding, L, *et al.* Integrated provenance and tectonic
975 implications of the Cretaceous–Palaeocene clastic sequence, Changla Gali, Lesser
976 Himalaya, Pakistan. *Geological Journal*. 2021; **56**(9): 4747-59.
- 977 68. Gaina, C, van Hinsbergen, DJJ, Spakman, W. Tectonic interactions between India
978 and Arabia since the Jurassic reconstructed from marine geophysics, ophiolite geology,
979 and seismic tomography. *Tectonics*. 2015; **34**(5): 875-906.
- 980 69. Gnos, E, Khan, M, Mahmood, K, *et al.* Bela oceanic lithosphere assemblage and
981 its relation to the Reunion hotspot. *Terra Nova*. 1998; **10**(2): 90-5.
- 982 70. Robinson, DM, DeCelles, PG, Copeland, P. Tectonic evolution of the Himalayan
983 thrust belt in western Nepal: Implications for channel flow models. *Geological Society of
984 America Bulletin*. 2006; **118**(7-8): 865-85.
- 985 71. Beaumont, C, Jamieson, RA, Nguyen, M, *et al.* Himalayan tectonics explained by
986 extrusion of a low-viscosity crustal channel coupled to focused surface denudation.
987 *Nature*. 2001; **414**(6865): 738-42.
- 988 72. Jagoutz, O, Bouilhol, P, Schaltegger, U, *et al.* The isotopic evolution of the
989 Kohistan Ladakh arc from subduction initiation to continent arc collision. *Geological
990 Society, London, Special Publications*. 2019; **483**(1): 165-82.
- 991 73. Orme, DA. Burial and exhumation history of the Xigaze forearc basin, Yarlung
992 suture zone, Tibet. *Geoscience Frontiers*. 2019; **10**(3): 895-908.
- 993 74. Einsele, G, Liu, B, Dürr, S, *et al.* The Xigaze forearc basin: evolution and facies
994 architecture (Cretaceous, Tibet). *Sedimentary Geology*. 1994; **90**(1-2): 1-32.
- 995 75. Huang, W, van Hinsbergen, DJJ, Maffione, M, *et al.* Lower Cretaceous Xigaze
996 ophiolites formed in the Gangdese forearc: Evidence from paleomagnetism, sediment
997 provenance, and stratigraphy. *Earth and Planetary Science Letters*. 2015; **415**: 142-53.
- 998 76. Yin, A, Harrison, TM, Ryerson, F, *et al.* Tertiary structural evolution of the
999 Gangdese thrust system, southeastern Tibet. *Journal of Geophysical Research: Solid
1000 Earth*. 1994; **99**(B9): 18175-201.
- 1001 77. Maffione, M, van Hinsbergen, DJJ, Koornneef, LMT, *et al.* Forearc
1002 hyperextension dismembered the south Tibetan ophiolites. *Geology*. 2015; **43**(6): 475-8.
- 1003 78. Li, Y, Li, R, Robinson, P, *et al.* Detachment faulting in the Xigaze ophiolite
1004 southern Tibet: New constraints on its origin and implications. *Gondwana Research*.
1005 2021; **94**: 44-55.
- 1006 79. Yin, A, Harrison, TM. Geologic evolution of the Himalayan-Tibetan orogen.
1007 *Annual Review of Earth and Planetary Sciences*. 2000; **28**(1): 211-80.
- 1008 80. Murphy, MA, Yin, A, Harrison, TM, *et al.* Did the Indo-Asian collision alone
1009 create the Tibetan plateau? *Geology*. 1997; **25**(8).
- 1010 81. Li, S, van Hinsbergen, DJ, Najman, Y, *et al.* Does pulsed Tibetan deformation
1011 correlate with Indian plate motion changes? *Earth and Planetary Science Letters*. 2020;
1012 **536**: 116144.
- 1013 82. Cowgill, E. Cenozoic right-slip faulting along the eastern margin of the Pamir
1014 salient, northwestern China. *Geological Society of America Bulletin*. 2010; **122**(1-2):
1015 145-61.
- 1016 83. Bullen, M, Burbank, D, Garver, J. Building the northern Tien Shan: Integrated
1017 thermal, structural, and topographic constraints. *The Journal of Geology*. 2003; **111**(2):
1018 149-65.

- 1019 84. Xiao, G, Guo, Z, Dupont-Nivet, G, *et al.* Evidence for northeastern Tibetan
1020 Plateau uplift between 25 and 20 Ma in the sedimentary archive of the Xining Basin,
1021 Northwestern China. *Earth and Planetary Science Letters*. 2012; **317**: 185-95.
- 1022 85. DeCelles, PG, Kapp, P, Quade, J, *et al.* Oligocene-Miocene Kailas basin,
1023 southwestern Tibet: Record of postcollisional upper-plate extension in the Indus-Yarlung
1024 suture zone. *Geological Society of America Bulletin*. 2011; **123**(7-8): 1337-62.
- 1025 86. Leary, R, Orme, DA, Laskowski, AK, *et al.* Along-strike diachroneity in
1026 deposition of the Kailas Formation in central southern Tibet: Implications for Indian slab
1027 dynamics. *Geosphere*. 2016; **12**(4): 1198-223.
- 1028 87. Li, S, Advokaat, EL, van Hinsbergen, DJJ, *et al.* Paleomagnetic constraints on the
1029 Mesozoic-Cenozoic paleolatitudinal and rotational history of Indochina and South China:
1030 Review and updated kinematic reconstruction. *Earth-Science Reviews*. 2017; **171**: 58-77.
- 1031 88. Bagheri, S, Gol, SD. The Eastern Iranian Orocline. *Earth-Science Reviews*. 2020:
1032 103322.
- 1033 89. Coleman, M, Hodges, K. Evidence for Tibetan plateau uplift before 14 Myr ago
1034 from a new minimum age for east–west extension. *Nature*. 1995; **374**(6517): 49-52.
- 1035 90. Gan, W, Molnar, P, Zhang, P, *et al.* Initiation of clockwise rotation and eastward
1036 transport of southeastern Tibet inferred from deflected fault traces and GPS observations.
1037 *GSA Bulletin*. 2021.
- 1038 91. Taylor, M, Yin, A. Active structures of the Himalayan-Tibetan orogen and their
1039 relationships to earthquake distribution, contemporary strain field, and Cenozoic
1040 volcanism. *Geosphere*. 2009; **5**(3): 199-214.
- 1041 92. Clark, MK, Royden, LH. Topographic ooze: Building the eastern margin of Tibet
1042 by lower crustal flow. *Geology*. 2000; **28**(8).
- 1043 93. van Hinsbergen, DJJ, Spakman, W, de Boorder, H, *et al.* Arc-type magmatism
1044 due to continental-edge plowing through ancient subduction-enriched mantle.
1045 *Geophysical Research Letters*. 2020; **47**(9): e2020GL087484.
- 1046 94. Shen, T, Wang, G, Replumaz, A, *et al.* Miocene subsidence and surface uplift of
1047 southernmost Tibet induced by Indian subduction dynamics. *Geochemistry, Geophysics,*
1048 *Geosystems*. 2020; **21**(10): e2020GC009078.
- 1049 95. Capitanio, FA, Morra, G, Goes, S, *et al.* India–Asia convergence driven by the
1050 subduction of the Greater Indian continent. *Nature Geoscience*. 2010; **3**(2): 136-9.
- 1051 96. Vaes, B, Gallo, LC, van Hinsbergen, DJ. On pole position: causes of dispersion of
1052 the paleomagnetic poles behind apparent polar wander paths. *Earth and Space Science*
1053 *Open Archive*. 2022; **preprint**.
- 1054 97. Saylor, JE, Sundell, KE. Quantifying comparison of large detrital geochronology
1055 data sets. *Geosphere*. 2016; **12**(1): 203-20.
- 1056 98. Wei, SS, Shearer, PM, Lithgow-Bertelloni, C, *et al.* Oceanic plateau of the
1057 Hawaiian mantle plume head subducted to the uppermost lower mantle. *Science*. 2020;
1058 **370**(6519): 983-7.
- 1059 99. Amaru, M. *Global travel time tomography with 3-D reference models*: Utrecht
1060 University; 2007.
- 1061 100. Torsvik, TH, Van der Voo, R, Preeden, U, *et al.* Phanerozoic polar wander,
1062 palaeogeography and dynamics. *Earth-Science Reviews*. 2012; **114**(3-4): 325-68.

1063

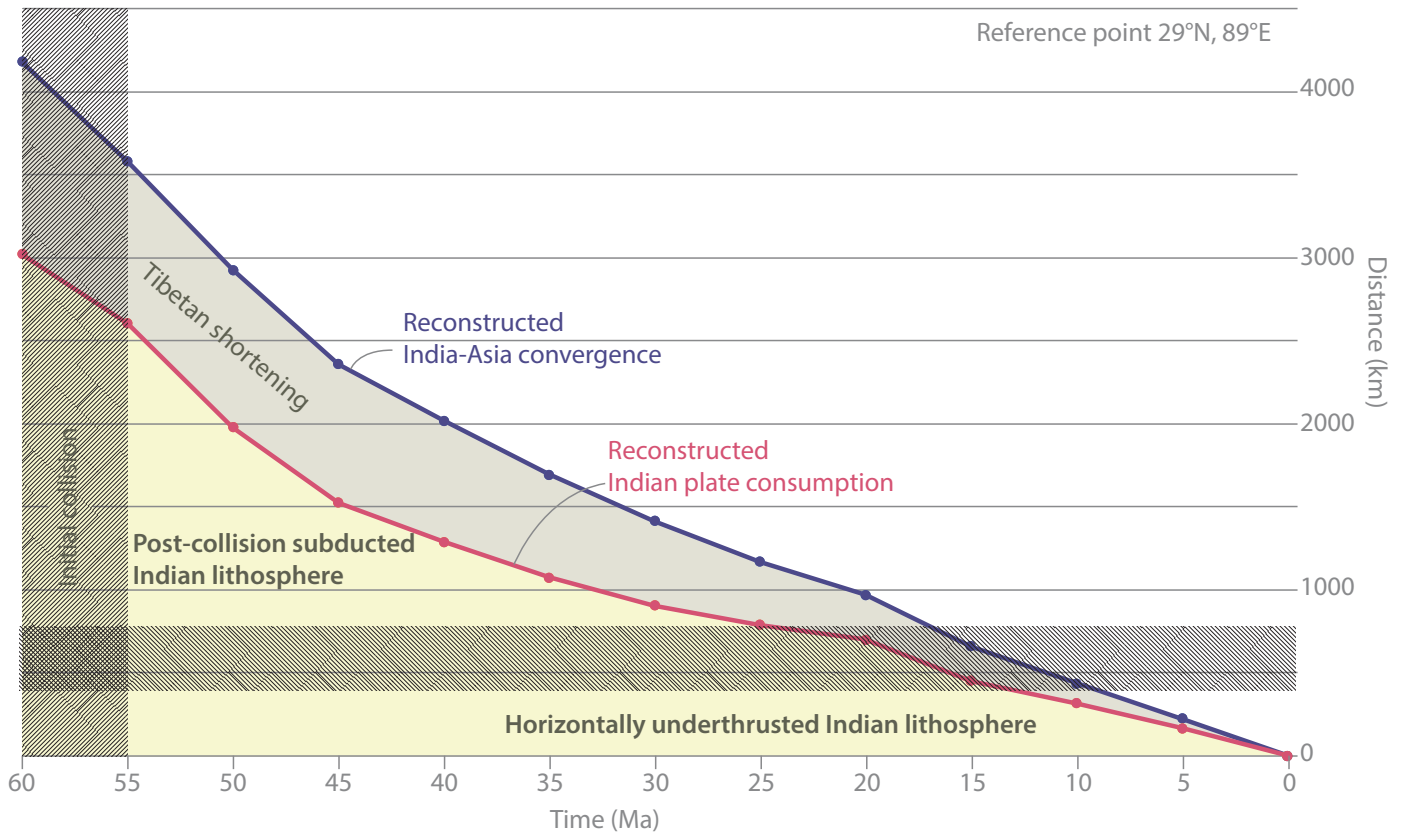


Figure 1

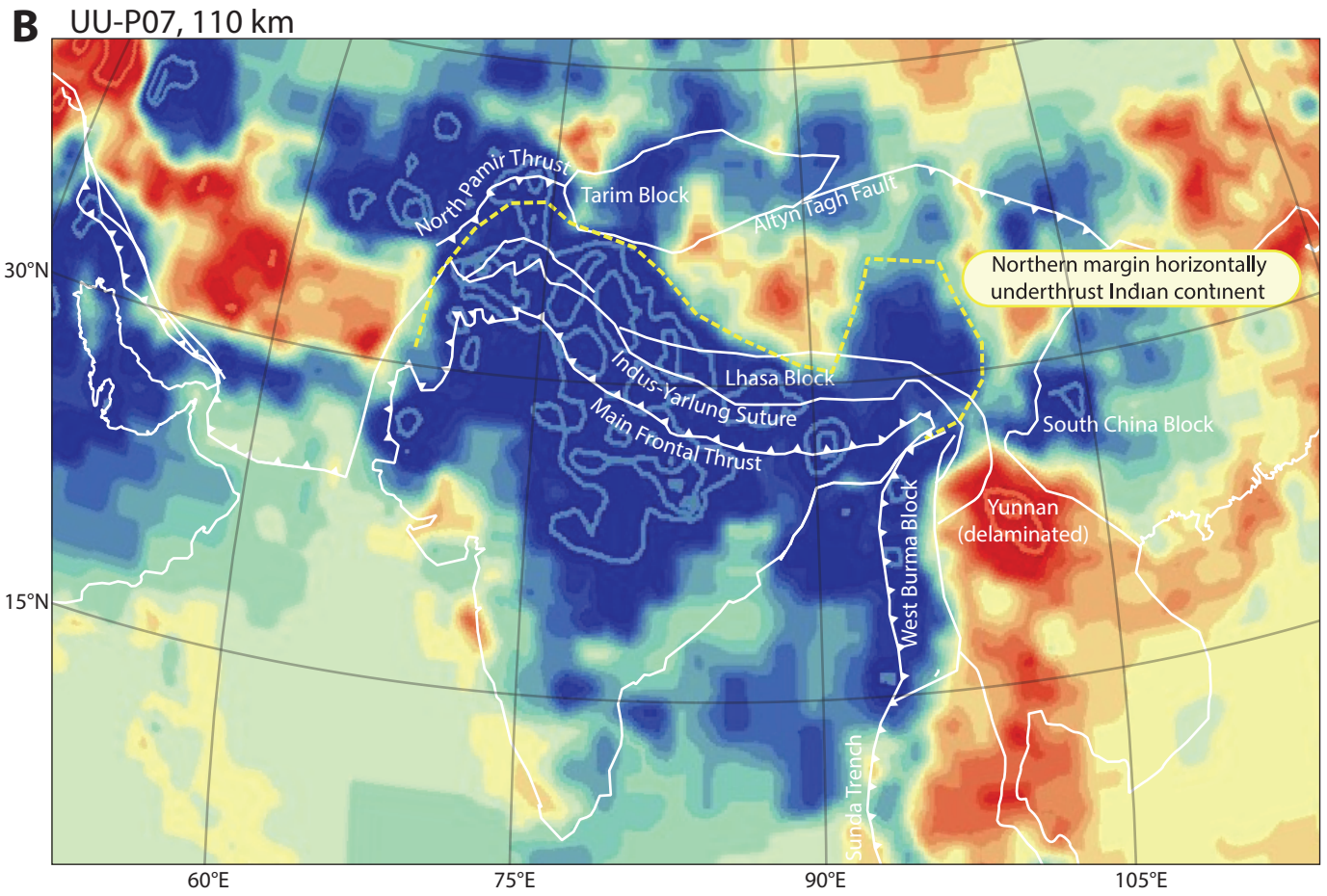
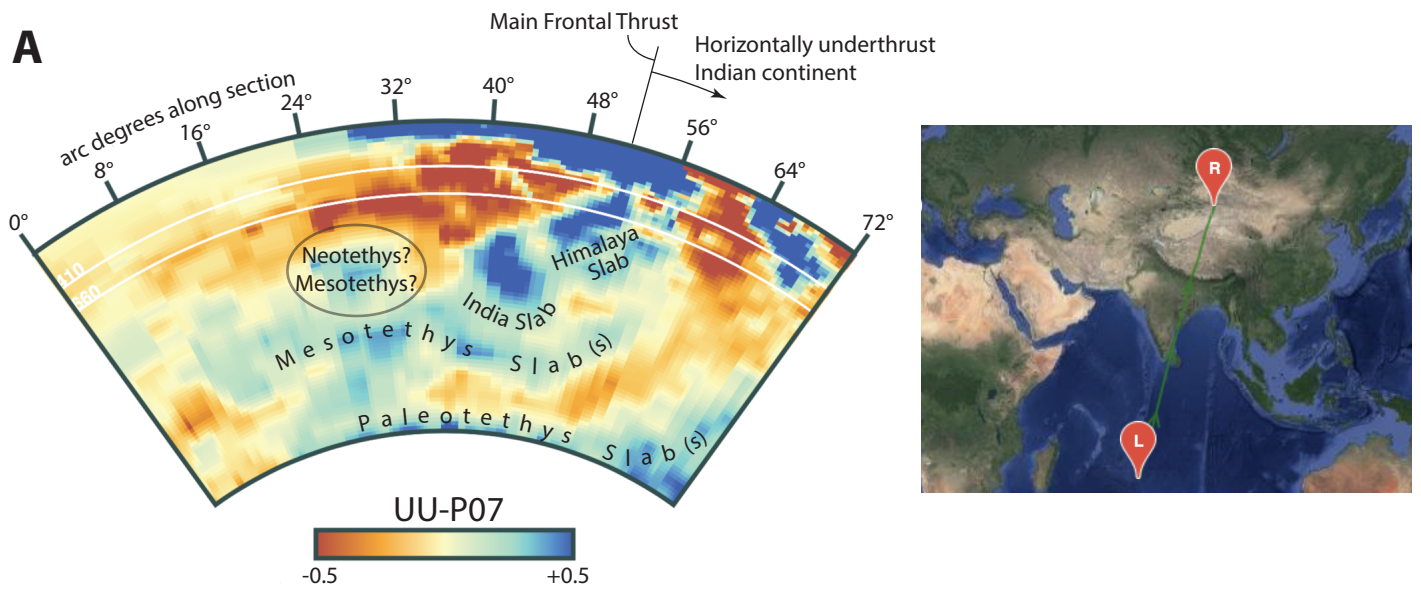


Figure 2

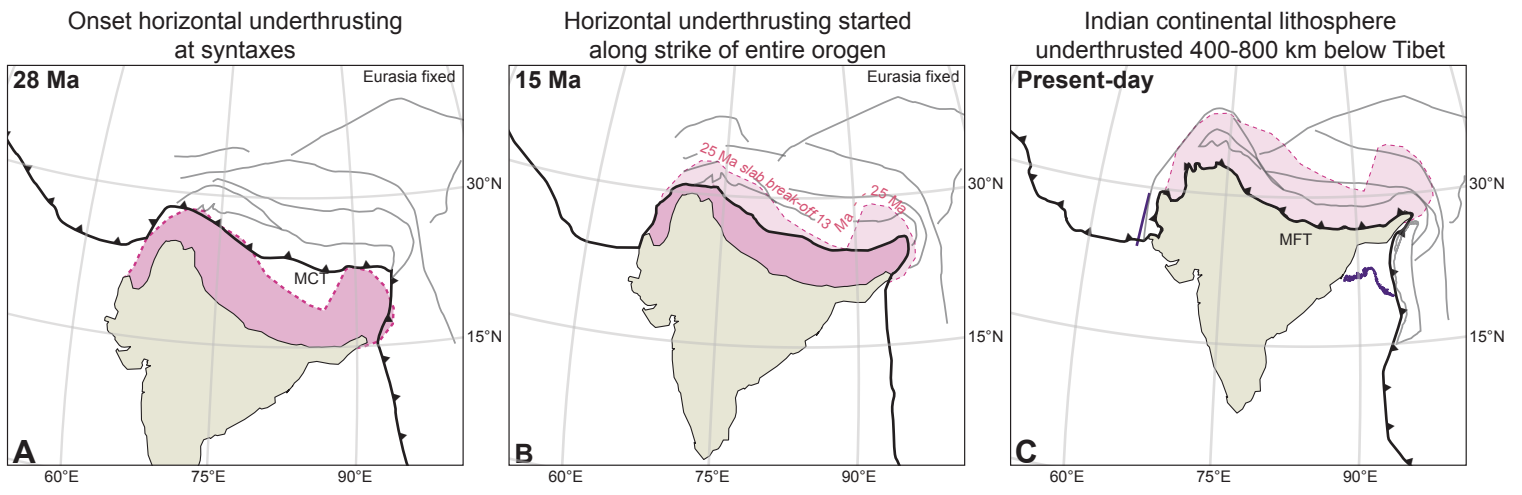


Figure 3

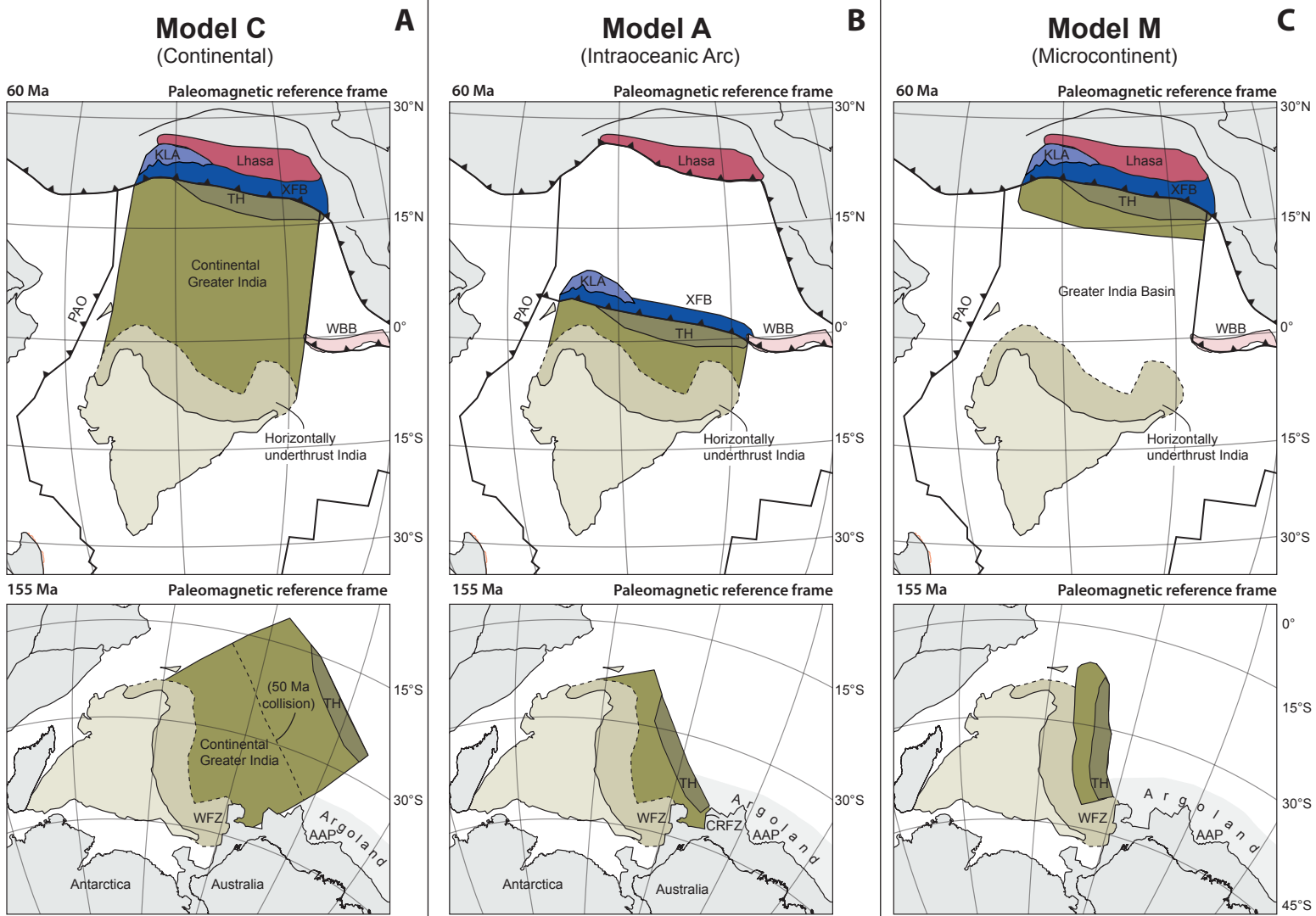


Figure 4

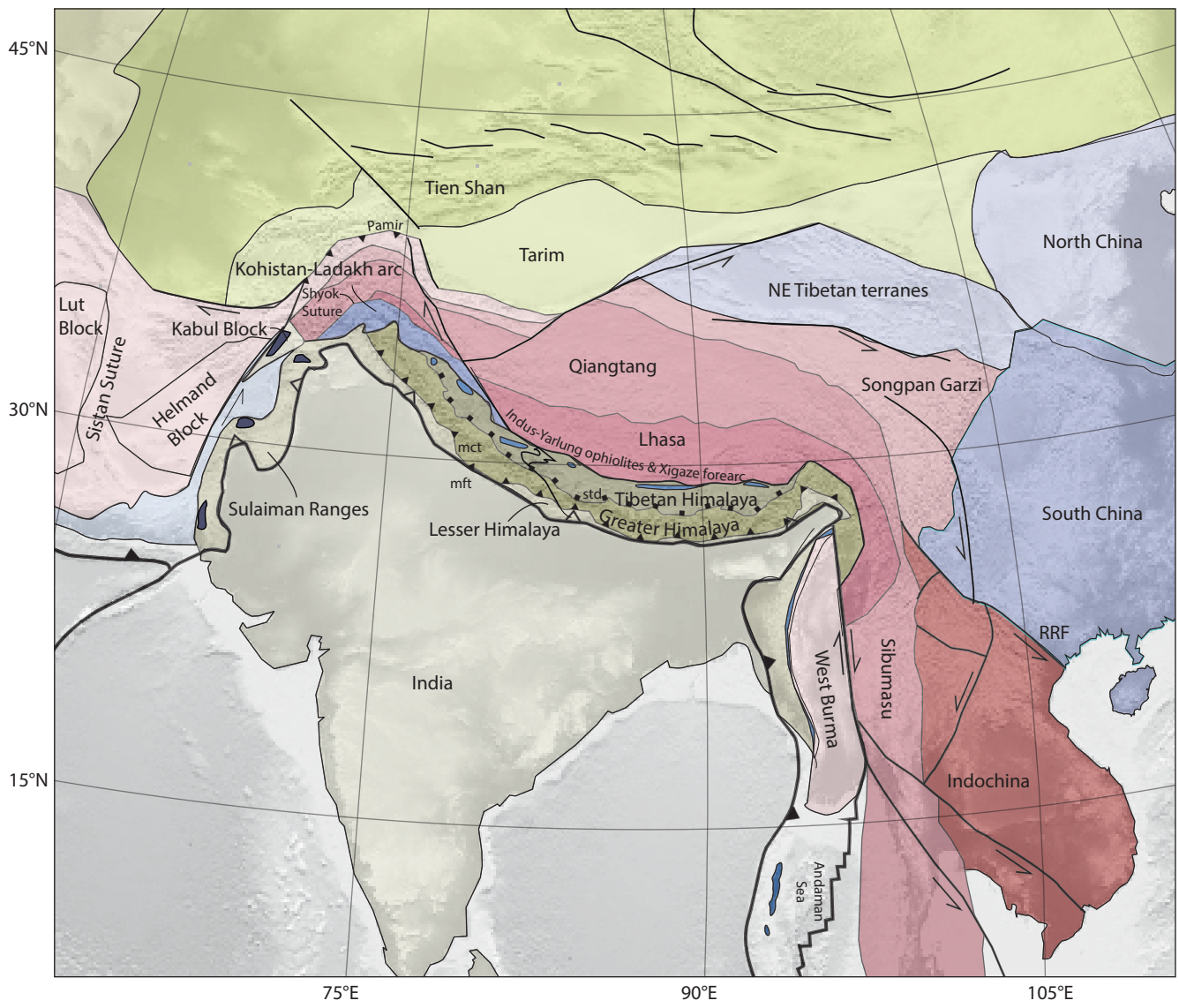


Figure 5

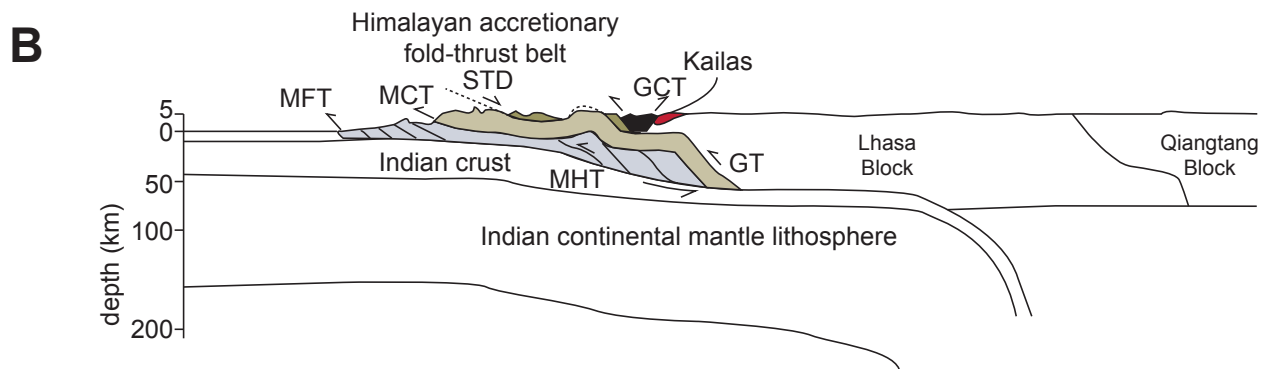
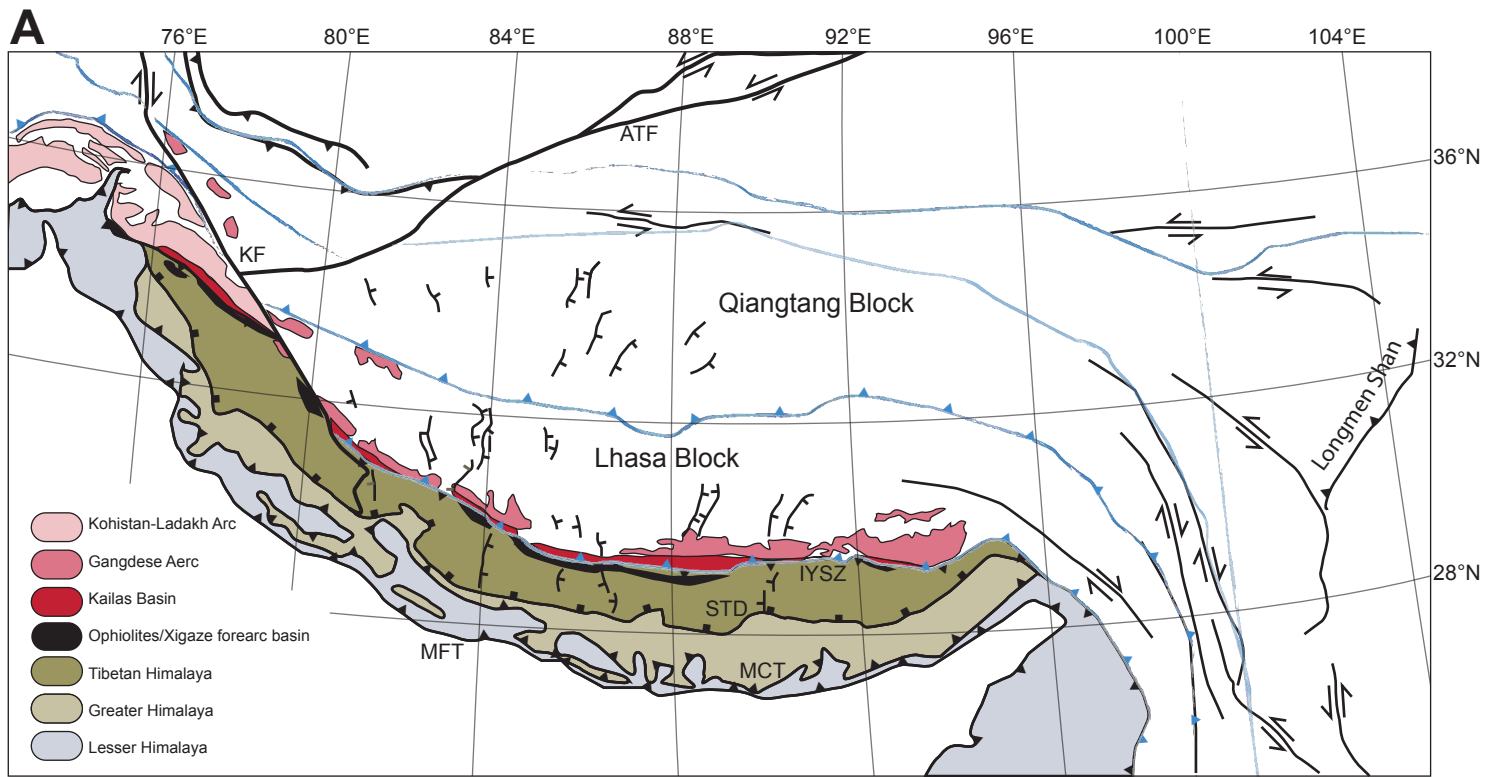
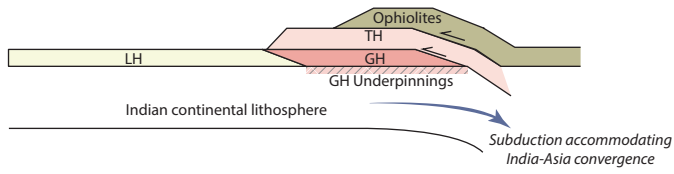


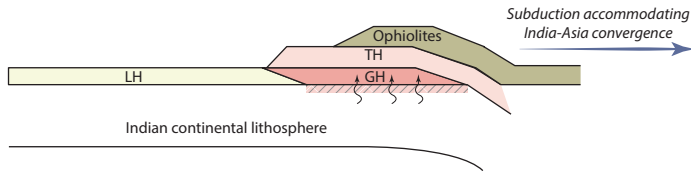
Figure 6

A. Eocene-Miocene India-Asia convergence accommodated to the north of the Himalaya

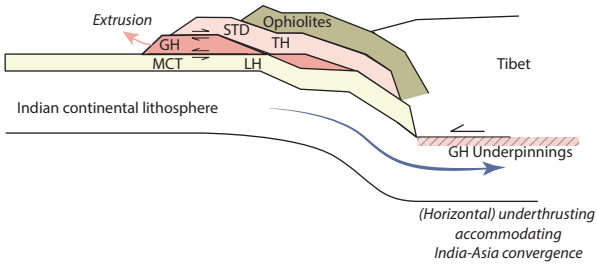
Late Paleocene-Early Eocene



Early Eocene-Early Miocene

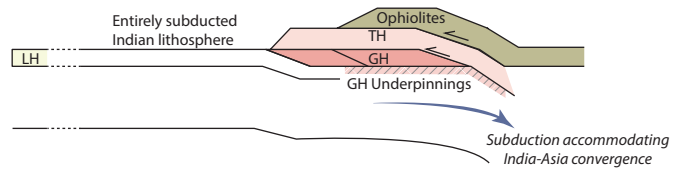


Early-Middle Miocene

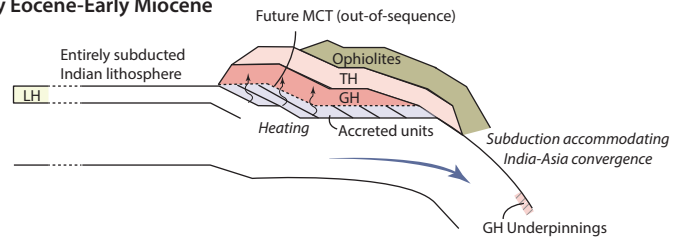


B. Eocene-Miocene India-Asia convergence (partly) accommodated within the Himalaya

Late Paleocene-Early Eocene



Early Eocene-Early Miocene



Early-Middle Miocene

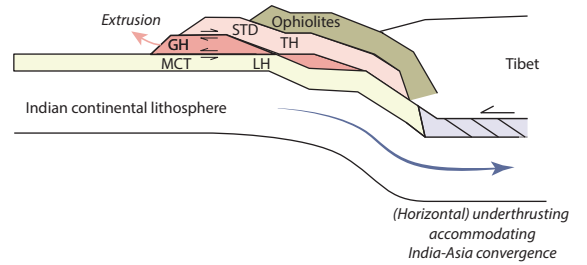


Figure 7

Miocene diachronous slab detachment and onset of horizontal underthrusting below Tibet

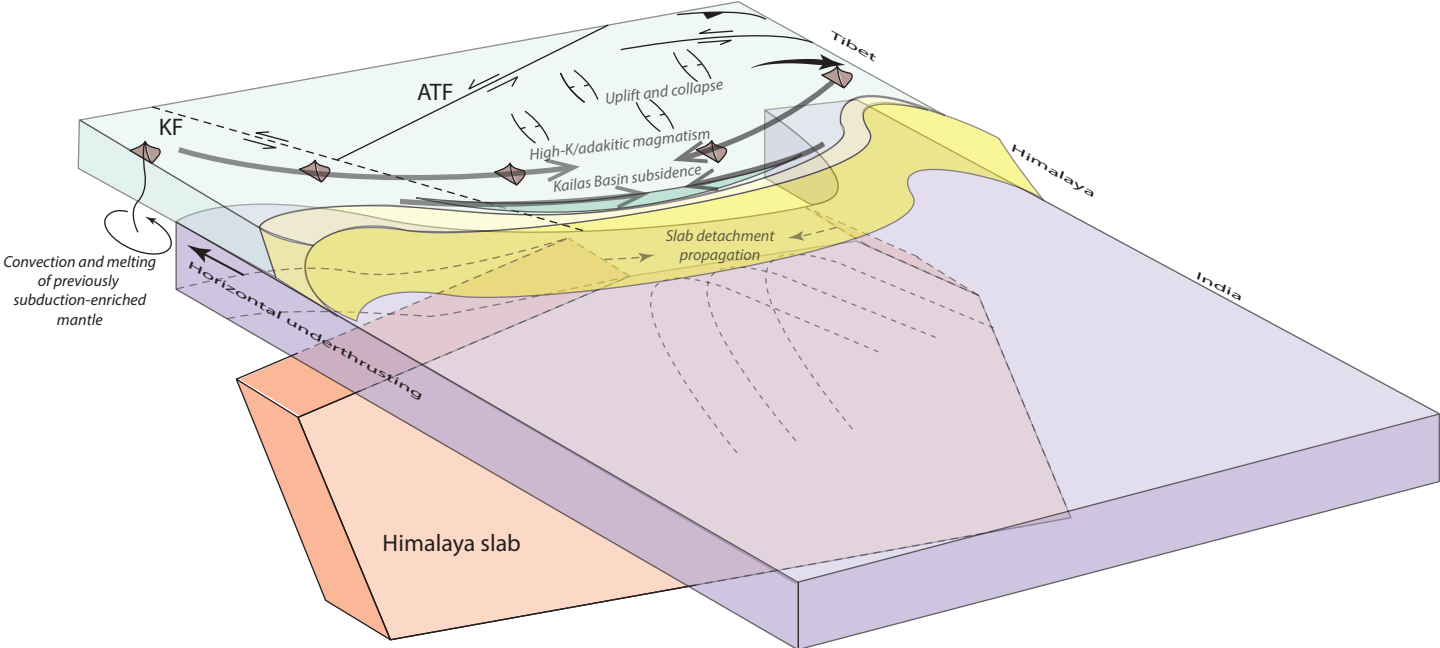


Figure 8